The Stepwise Reduction of Multiyear Sea Ice Area in the Arctic Ocean Since 1980.

D.G. Babb[1,2] (David.Babb@umanitoba.ca) (ORCID: 0000-0002-7427-8094)
R.J. Galley[2,3] (ORCID: 0000-0002-5403-9694)
S. Kirillov[1] (ORCID: 0000-0002-9636-7952)
J.C. Landy[4] (ORCID: 0000-0002-7372-1007)
S.E.L. Howell[5] (ORCID: 0000-0002-4848-9867)
J.C. Stroeve[1,2,6,7] (ORCID: 0000-0001-7316-8320)
W. Meier[7] (ORCID: 0000-0003-2857-0550)
J.K. Ehn[1,2] (ORCID: 0000-0002-8885-7441)
D.G. Barber[1,2] †

[1] Centre for Earth Observation Science, University of Manitoba, Winnipeg, MB, Canada
[2] Department of Environment and Geography, University of Manitoba, Winnipeg, MB, Canada
[3] Department of Fisheries and Oceans Canada, Winnipeg, MB, Canada.
[4] Department of Physics and Technology, UiT The Arctic University of Norway, Tromsø, Norway
[5] Environment and Climate Change Canada, Toronto, ON, Canada
[6] Department of Earth Sciences, University College London, London, United Kingdom
[7] National Snow and Ice Data Center, Cooperative Institute for Research in Environmental Sciences at the University of Colorado Boulder, Boulder, Colorado, United States

† Deceased April 15, 2022

Key Points:

1. Multiyear sea ice (MYI) loss from the Arctic Ocean has primarily occurred through two stepwise reductions; 1989 and 2006-2008.
2. 1989 was the result of high MYI export, while 2006-2008 was the result of high MYI export and melt, and limited MYI replenishment.
3. Though presently stable, reduced retention to older MYI has created a younger thinner MYI pack that may be conditioned for another reduction.

Abstract:

The loss of multiyear sea ice (MYI) in the Arctic Ocean is a significant change that affects all facets of the Arctic environment. Using a lagrangian ice age product we examine MYI loss and quantify the annual MYI area budget from 1980-2021 as the balance of export, melt and replenishment. Overall, MYI area declined at 72,500 km^2/yr, however a majority of the loss occurred during two stepwise reductions that interrupt an otherwise balanced budget and resulted in the northward contraction of the MYI pack. First, in 1989, a change in atmospheric forcing led to a +56% anomaly in MYI export through Fram Strait. The second occurred from 2006-2008 with anomalously high melt (+25%) and export (+23%) coupled with low replenishment (-8%). In terms of trends, melt has increased since 1989, particularly in the Beaufort Sea, export has decreased since 2008 due to reduced MYI coverage north of Fram Strait, and replenishment has increased over the full time series due to a negative feedback that promotes seasonal ice survival at higher latitudes exposed by MYI loss. However, retention to older MYI has significantly declined, transitioning the MYI pack towards younger MYI that is less resilient than previously anticipated and could soon elicit another stepwise reduction. We speculate that future MYI loss will be driven by increased melt and reduced replenishment, both of which are enhanced with continued warming and will one day render the Arctic Ocean free of MYI, a change that will coincide with a seasonally ice-free Arctic Ocean.

Plain Language Summary:

Sea ice that has survived through at least one melt season is referred to as multiyear sea ice. It is inherently thicker, has a higher albedo and is overall more resilient to melt than seasonal sea ice. Historically, multiyear ice covered a vast majority of the Arctic Ocean, however its areal extent has declined and transitioned the Arctic ice pack to a younger state that is more susceptible to melt. To this point the loss of multiyear ice is known, but it remains unclear whether it was a change in multiyear ice loss through export or melt or the source of multiyear through replenishment that has driven this change. By quantifying these three terms for each of the past 42 years we find that multiyear ice loss primarily occurred through two stepwise reductions, with the budget otherwise generally being in balance. The first loss occurred in 1989 due to anomalously high export, while the second loss occurred between 2006 and 2008 through a confluence of anomalously high export and melt and low replenishment. Trends of reduced export, increased melt and increased replenishment, and overall negative multiyear ice balance, suggest the eventual disappearance of multiyear ice from the Arctic Ocean.

1. Introduction:

The loss of multiyear sea ice (MYI) and transition to a predominantly first year sea ice (FYI) cover is one of the most dramatic changes taking place in a warming Arctic (Comiso, 2012; Constable et al., 2022; Kwok, 2018; Maslanik et al., 2011; Meier et al., 2021; Meredith et al., 2019; Nghiem et al., 2011; Stroeve & Notz, 2018; Tschudi et al., 2016). MYI is defined as sea ice that has survived at least one melt season, and ages as it survives through additional melt seasons. MYI is inherently thicker than FYI due to accumulated deformation and continued thermodynamic ice growth (Kwok, 2004a), and it has a higher albedo due to greater snow accumulation, a surface scattering layer and reduced melt pond coverage (Perovich & Polashenski, 2012). As a result, MYI is more robust and resilient to summer melt than FYI, and thus forms the backbone of the Arctic ice pack through the melt season with the end of winter MYI edge being a prognosticator of the annual minimum sea ice extent (Thomas & Rothrock, 1993). As the Arctic has warmed, the MYI pack has declined in area (Comiso, 2012; Kwok, 2018; Maslanik et al., 2011) and thickness (Kacimi & Kwok, 2022; Kwok et al., 2009; Petty et al., 2023) weakening the backbone of the Arctic ice pack and making it more susceptible to further reductions. MYI loss represents a significant shift in the Arctic environment that has implications for the Arctic ecosystem, the global climate system, industrial and transportation related interests in the north and most importantly for Inuit who live in the Arctic and rely on the marine environment (Constable et al., 2022; Meredith et al., 2019).

Historically, MYI covered a vast majority of the Arctic Ocean. A portion was exported annually through Fram Strait via the Transpolar Drift Stream while the majority was redistributed and retained within the Beaufort Gyre for more than 10 years (Rigor & Wallace, 2004). In the 1950s and 1960s the end-of-winter MYI extent was approximately 5.5×10^6 km^2 (Nghiem et al., 2007). Beginning in the 1970s, the end-of-winter MYI extent decreased at a rate of 0.5×10^6 km^2 per decade and fell to approximately 4×10^6 km^2 by the end of the 20th century (Nghiem et al., 2007). MYI loss accelerated through the 2000s (Comiso, 2012) with a dramatic reduction in MYI area of 1.54×10^6 km^2 between 2005 and 2008 (Kwok et al., 2009), and a current record minimum of 1.6×10^6 km^2 at the end-of-winter 2017 (Kwok, 2018). Despite significant negative linear trends in MYI area, Comiso et al., (2012) found an 8-9 year cycle in MYI area, with years of loss followed by recovery.

Similarly, Regan et al., (2023) found that between 2000 and 2018 modeled MYI area declined through episodic losses in 2007 and 2012.

The reduction in MYI area coincides with the reduction in Arctic sea ice thickness that has occurred since the original observations of thickness were collected beneath a primarily MYI cover by submarines in the 1950s and 1960s (Bourke & Garret, 1987; Kwok & Rothrock, 2009; Rothrock et al., 1999). Ice thickness and age have been found to be positively correlated, with thickness increasing between 0.19 m yr^{-1} (Maslanik et al., 2007) and 0.36 m yr^{-1} (Tschudi et al., 2016). As a result, from 2003 to 2018, MYI area and winter sea ice volume were strongly correlated (R^2 = 0.85; Kwok, 2018). Overall, the reduction in MYI area has strongly contributed to the reduction in sea ice thickness within the Arctic Ocean.

Annual changes in MYI area within the Arctic Ocean reflect a balance between MYI loss through export and melt, and replenishment, which is FYI that survives through the melt season and is the sole source of MYI. To-date MYI export, replenishment, and melt have been examined in different works over different periods of time and for different regions (i.e. Babb et al., 2022; Howell et al., 2023; Kuang et al., 2022; Kwok, 2004b, 2007, 2009; Kwok et al., 2009; Kwok & Cunningham, 2010; Ricker et al., 2018), yet they have not been coherently analyzed to produce a long-term MYI budget of the Arctic Ocean and examine MYI loss. Regan et al., (2023) recently examined MYI area and volume loss from 2000-2018 in terms of MYI export, melt, replenishment and ridging using the neXtSIM ice-ocean model, yet the model performs poorly during some years (i.e. 2016; Boutin et al., 2023) and is limited to an 18 year period at which point MYI had already declined considerably. In this paper we use 43 years of remotely sensed fields of sea ice motion, age and concentration to examine the MYI area budget of the Arctic Ocean. We use the relative changes and contributions of export, melt, and replenishment to understand what has driven the dramatic loss of MYI and what the future holds for MYI in the Arctic Ocean.

2. Background of the MYI Budget Terms

2.1 MYI Export

MYI can be exported across any of the open boundaries of the Arctic Ocean, though it is primarily exported through Fram Strait (87%; Kuang et al., 2022). A lesser amount is

exported seasonally into Nares Strait (Howell et al., 2023; Kwok, 2005; Kwok et al., 2010; Moore, Howell, Brady, et al., 2021) and into the Queen Elizabeth Islands (QEI) of the CAA (Howell et al., 2023; Howell & Brady, 2019), while MYI has occasionally been exported into the Barents Sea (Kwok et al., 2005) and through the Bering Strait (Babb et al., 2013).

Estimates of annual total ice (MYI and FYI) area export through Fram Strait vary from 706,000 km^2 (Kwok, 2009) to 880,000 km^2 (Smedsrud et al., 2017), yet the proportion of MYI varies according to the orientation of the Transpolar Drift Stream, which advects sea ice towards Fram Strait. An eastward shift in the Transpolar Drift Stream results in more FYI export from the Russian Seas, whereas a westward shift results in older ice being more readily drawn out of the Beaufort Gyre (Hansen et al., 2013; Kwok, 2009; Pfirman et al., 2004). The orientation of the Transpolar Drift Stream is dictated by the surface pressure patterns over the Arctic Ocean that are characterized by the Arctic Oscillation (AO) index. The negative phase of the AO shifts the Transpolar Drift Stream to the east, while the positive phase shifts the Transpolar Drift Stream to the west (Rigor et al., 2002). The shift from a prolonged negative AO to a positive AO in the late 1980s led to a "flushing" of MYI out of the Beaufort Gyre into the Transpolar Drift Stream and through Fram Strait (Pfirman et al., 2004). This flushing event is thought to have caused a permanent shift in the thickness and concentration of the Arctic ice pack (Lindsay & Zhang, 2005), a shift which ultimately conditioned it for the record minimum of 2007 (Lindsay et al., 2009).

In terms of the proportion of MYI passing through Fram Strait, Gow and Tucker (1987) reported that 84% of the ice in Fram Strait during summer 1984 was MYI, while Kwok and Cunningham (2015) assumed 70% during winters (October to April) 2011-2014. More recently, Ricker et al. (2018) used the sea ice type product (OSI-403) from the EUMETSAT Ocean and Sea Ice Satellite Application Facility (OSISAF) to estimate a MYI proportion between 64% and 94% during winters 2010-2017. Using the estimate of 706,000 km^2 of total ice export and the range in MYI proportion presented by Ricker et al. (2018), Babb et al. (2022) estimated that 453,000-660,000 km^2 of MYI was exported annually through Fram Strait. More recently, Wang et al., (2022) used another remotely sensed ice type product (ECICE; Shokr et al., 2008) to determine that on average 343,000 km^2 of MYI was exported through Fram Strait during winter between 2002 and 2020.

Given that approximately 87% of the annual ice export through Fram Strait occurs during winter (Kwok, 2009), we scale the results of Wang et al., (2022) to an annual average MYI export of 388,000 km^2. However, Wang et al., (2022) note that MYI export through Fram Strait declined by 22% between the first and second half of their study period, due to a reduction in MYI transport from the Beaufort Sea and Siberian coast towards Fram Strait and therefore younger ice in the Transpolar Drift Stream (i.e. Comiso, 2012; Haas et al., 2008; Hansen et al., 2013; Krumpen et al., 2019; Sumata et al., 2023). Reduced MYI export aligns with the observed decrease in sea ice volume export through Fram Strait since the 1990s (Sumata et al., 2022).

MYI export into Nares Strait and the QEI is an order of magnitude lower than MYI export through Fram Strait, yet export is increasing through both channels. This is particularly important because the oldest and thickest MYI in the Arctic is exported through these channels (Howell et al., 2023; Kwok et al., 2010; Moore et al., 2019). Furthermore, increasing MYI export through these channels has implications for ships operating downstream along the Northwest Passage (Howell et al., 2022; Pizzolato et al., 2014) and as far south as Newfoundland (Barber et al., 2018). Ice export through these channels is limited by the seasonal formation of ice arches (also known as ice bridges or barriers; Hibler et al., 2006; Kirillov et al., 2021; Melling, 2002) that impede ice motion, yet as the Arctic warms these arches are forming for shorter periods and occasionally not forming at all, allowing increased ice export (Howell et al., 2023; Howell & Brady, 2019; Moore, Howell, Brady, et al., 2021). Annual ice export into Nares Strait increased from 33,000 km^2 between 1996-2002 (Kwok, 2005) to 87,000 km^2 between 2019-2021 (Moore, Howell, Brady, et al., 2021) and more recently 95,000 km^2 between 2017-2021 (Howell et al., 2023). Meanwhile annual ice export into the QEI increased from 8,000 km^2 between 1997-2002 (Kwok, 2006) to 25,000 km^2 between 1997-2018 (Howell & Brady, 2019), with a recent peak of 120,000 km^2 in 2020 (Howell et al., 2023). Assuming a MYI proportion of 50% in Nares Strait and 100% in the QEI, Babb et al., (2022) used the average total ice export of Moore et al., (2021)and Howell and Brady (2019) to estimate an annual average MYI export of 68,500 km^2 through these channels. However, Howell et al., (2023) show that between 2017 and 2021 an average of 113,200 km^2 of MYI was exported annually through these channels, which far exceeds the estimates of Babb et al., (2022) and is 29% of the

193 estimated annual average MYI export through Fram Strait between 2002 and 2020 (Wang
194 et al., 2022). Overall, MYI export into Nares Strait and the QEI is increasing in magnitude
195 and playing a greater role in the overall MYI budget of the Arctic Ocean.
196
197 **2.2 MYI Melt**
198 Traditionally, very little MYI was thought to completely melt within the Arctic Ocean
199 (Kwok & Cunningham, 2010) as lateral melt of MYI floes was assumed to be negligible
200 when examining annual records of MYI area (Kwok, 2004a). However, Kwok and
201 Cunningham (2010) found that export alone could not satisfy the dramatic reduction of
202 MYI area in the early 2000s, highlighting the increasing contribution of melt. Although MYI
203 can melt in any area of the Arctic Ocean there has been a focus on MYI melt within the
204 Beaufort Sea because of its broader role of retaining MYI within the Beaufort Gyre (Kwok
205 and Cunningham, 2010; Babb et al., 2022). Between 1981 and 2005, 93% of MYI passing
206 through the Beaufort Sea survived through the melt season, facilitating the redistribution
207 of MYI via the Gyre and maintaining a relatively high MYI area in the Arctic Ocean
208 (Maslanik et al., 2011). However, an accelerated ice-albedo feedback increased ice melt in
209 the Beaufort Sea through the 2000s (i.e. Perovich et al., 2008), which led to reductions in
210 MYI thickness (Krishfield et al., 2014; Mahoney et al., 2019) and increased MYI loss (Kwok
211 and Cunningham, 2010; Babb et al., 2022). As a result, between 2006 and 2010 the survival
212 rate of MYI passing through the Beaufort Sea declined to 73% (Maslanik et al., 2011), with
213 approximately one-third of the pan-Arctic MYI loss between 2005 and 2008 being lost to
214 melt in the Beaufort Sea (Kwok and Cunningham, 2010). Using a regional MYI budget, Babb
215 et al., (2022) found that MYI melt in the Beaufort Sea quadrupled between 1997 and 2021,
216 interrupting MYI transport through the Beaufort Gyre and precluding MYI from being
217 advected onwards to other marginal seas. In particular, MYI melt in the Beaufort Sea
218 peaked at 385,000 km^2 in 2018, which is similar to the estimated magnitude of MYI export
219 through Fram Strait (Babb et al., 2022; Wang et al., 2022).
220
221 **2.3 MYI Replenishment**
222 As the sole source of MYI, annual replenishment of MYI from FYI that survives the
223 melt season is a critical yet understudied term in the MYI budget. The first estimates of MYI

replenishment were presented by Kwok (2004), who constructed annual cycles of MYI area in the Arctic Ocean by taking the MYI area determined by QuickSCAT on January 1 and then adjusting the area by the record of MYI export through Fram Strait. MYI replenishment was then calculated as the difference between the estimated MYI area during the September minimum (projected forwards from January 1) and the estimated MYI area in October (projected backwards from January 1). Using this method, replenishment averaged 1.1 x 10^6 km^2 from 2000-2002 (Kwok, 2004), though there was subsequently near-zero replenishment in 2005 (Kwok, 2007) and 2007 (Kwok et al., 2009).

Kwok (2007) found that ~63% of the variance in MYI replenishment from 2000-2006 was explained by a combination of melting-degree-day (MDD) anomalies during summer and freezing-degree-day (FDD) anomalies during the preceding winter. Generally, warmer temperatures during summer increase ice melt and reduce the likelihood of FYI surviving through summer and replenishing MYI, while colder temperatures during the preceding winter create thicker FYI that is more likely to persist through the melt season and replenish MYI. The importance of ice growth during the preceding winter reflects the negative conductive feedback; thin ice grows faster thermodynamically than existing thick ice, and thereby stabilizes the ice pack (Bitz & Roe, 2004; Notz, 2009). However, this feedback has weakened since 2012 due to the occurrence of warmer winters limiting thermodynamic ice growth (Stroeve et al., 2018), particularly in 2015 when an anomalously warm winter reduced FYI volume by 13% at the end of winter and was proposed to have limited MYI replenishment (Ricker et al., 2017). Ultimately, reduced FYI growth during winter not only encourages lower summer sea ice extents, but also limits MYI replenishment and therefore amplifies annual sea ice loss.

3. Data and Methods:

3.1 Ice Age Dataset

The basis for this analysis is the EASE-Grid Sea Ice Age dataset from the National Snow and Ice Data Center (NSIDC; Version 4 – Tschudi et al., 2019; updated 2021). The dataset provides weekly fields of ice age at 12.5 km resolution across the Arctic Ocean since 1984 and has previously been employed to highlight MYI loss (e.g. Meier et al., 2021; Stroeve & Notz, 2018), and validate other remotely sensed ice-type products (Ye et al.,

2023) and modelled MYI coverage (Jahn et al., 2012; Regan et al., 2023). The dataset estimates ice age by lagrangian parcel-tracking through the NSIDCs Polar Pathfinder Sea Ice Motion Dataset (Version 4 - Tschudi et al., 2019b; updated 2021) and determining how long a parcel persists. Parcels age by 1-year after the week of the September sea ice minimum so long as the concentration of the grid cell they are in remains above 15%. A similar method was used by Rigor and Wallace (2004) to estimate ice age from gridded ice motion fields derived from buoy tracks, though Nghiem et al. (2006) found that insufficient coverage of buoys at certain times introduced uncertainties in the ice age model. The Ice Age product overcomes this by integrating buoy tracks with daily fields of ice motion derived from spaceborne passive microwave radiometers, providing a continuous record of ice motion necessary to track parcels for years.

The passive microwave record and therefore the ice motion record began in October 1978, yet the Ice Age product requires time to spin up and develop an ice age distribution (up to 5 years), hence it has typically only been available since 1984. However, following the September sea ice minimum of 1979 MYI can be distinguished from FYI, hence our analysis of MYI begins in September 1979 using data available from Meier et al., (2023), but ice age distributions are only available since 1984.

One limitation of the Ice Age product is that each grid cell is assigned the age of the oldest parcel within it at that time, meaning that there is no partial MYI concentration like in ice charts (i.e. Babb et al., 2022) or other remotely sensed ice type products (i.e. Comiso, 2012; Kwok, 2004a). As a result there is an inherent overestimation of MYI area within the dataset (Korosov et al., 2018; Tschudi et al., 2016), an error that grows during fall freeze-up when grid cells with low MYI concentrations (>=15%) freeze-up completely with new ice but continue to be identified as MYI. Korosov et al., (2018) suggest that this overestimation is greater in the marginal ice zone than the central Arctic because there is a greater mixture of MYI and FYI around the periphery of the ice pack. Despite this limitation, the Ice Age product has the critical advantage of being available year-round, whereas other remotely sensed ice-type products are confined to the ice growth season because once the ice/snow surface begins to melt, distinguishing ice types becomes more uncertain.

3.2 MYI Budget

To examine the MYI budget of the Arctic Ocean we must define the boundaries, calculate the weekly time series of MYI area within the region (Figure 1), and calculate MYI export across the boundaries. Following Kwok (2004) the Arctic Ocean was defined by boundaries across Fram Strait, the channels between Svalbard, Franz Josef Land and Severnya Zemlya, the Bering Strait, the western edge of the CAA and the northern entrance to Nares Strait (Figure 2). MYI area in the Arctic Ocean was calculated by summing the weekly mean sea ice area in pixels identified as MYI within the weekly ice age dataset. Sea ice area was calculated from the NSIDC daily passive microwave sea ice concentration dataset (Cavalieri et al., 1996; updated 2022). MYI area is characterized by a well-defined annual cycle from a maximum following replenishment to the minimum during September with the decrease in MYI area being the result of export during winter and the combination of export and melt during summer (Figure 1A; Figure S1).

Critical to the annual cycle and definition of MYI is that MYI is only created by replenishment from FYI that survives through the minimum. Replenishment is calculated as the area of second year ice (MYI2) during the week after the minimum (Figure 1A). However, the time series of MYI area calculated from the Ice Age dataset shows an erroneous increase in MYI area after replenishment, which is the result of concentration increasing within pixels containing at least some portion of MYI during freeze-up. To account for this error we use a method similar to Kwok (2004) and create an estimated annual record of MYI area by accounting for MYI export (Figure 1B). We use the maximum and minimum MYI area to bookend the annual record and then account for MYI export across all of the Arctic Oceans boundaries to create a timeseries of estimated MYI area (dashed line Figure 1B). At the time of the September minimum we sum the net export for the ice season (blue line Figure 1B) and determine MYI melt as the difference between the estimated MYI area, which is based solely on export, and the calculated MYI area, which reflects MYI lost to export and melt (red line Figure 1B). Because MYI area is inherently overestimated within the Ice Age dataset, MYI export and the MYI minimum are overestimated, meaning that MYI melt and MYI replenishment are underestimated. To constrain this error we calculate the difference between the peak in the calculated MYI area and the estimated MYI area at that time (Figure 1B; Figure S1). On average 503,000 km^2 or 15% of the MYI area is erroneously created during freeze up, meaning that MYI export can

be overestimated by as much as 15%. However, based on the results of Korosov et al,. (2018), most of the error accrues in the marginal seas and has a lesser impact on MYI export, particularly through Fram Strait.

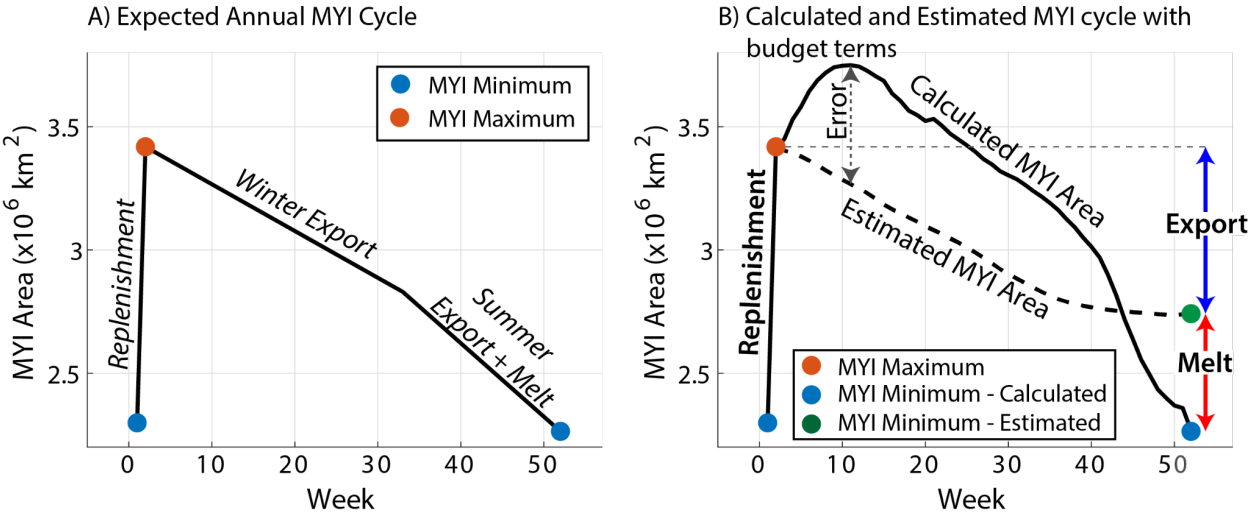

Figure 1: The Expected (A), and Calculated and Estimated (B), annual cycles of MYI Area in the Arctic Ocean, in weeks after the September minimum. Terms of the presented MYI budget are bolded in B.

An additional source of error in determining MYI area stems from the convergence/divergence of the MYI pack and specifically how this is handled in the Ice Age dataset. Theoretically, divergence has no impact on MYI area (area is conserved), whereas convergence leads to deformation which reduces MYI area but conserves MYI volume. Previous work on the annual MYI cycle has assumed that MYI does not deform (Kwok, 2004), or has acknowledged that it may deform but does not consider deformation as a sink of MYI area (Kwok and Cunningham, 2010). Regan et al., (2023) calculated MYI deformation as convergence of modeled ice motion fields, yet they assumed that FYI was preferentially deformed and the MYI deformation only occurred once all FYI had been deformed. Mimicking this with ice motion fields and the Ice Age dataset would introduce significant uncertainty and require additional tracking of each parcel of MYI to determine the actual MYI concentration and cumulative convergence over time. Given this uncertainty in quantifying MYI deformation, we do not account for this term within the MYI budget which may in turn lead to an overestimate of MYI melt.

Ice flux (F) across the boundaries of the Arctic Ocean is calculated at regular intervals using the following equation,

$$F = c\,u\,\Delta x \qquad (1)$$

where, c is the sea ice concentration, u is the ice velocity component normal to the gate and Δx is the interval. For large channels like Fram Strait, and channels into the Kara and Barents Seas, F was calculated weekly using fields of sea ice drift and concentration from the NSIDC datasets, and used to calculate MYI flux by summing points along the flux gate identified as MYI by the Ice Age dataset. Negative fluxes represent MYI export from the Arctic Ocean, while positive fluxes represent MYI import.

For the narrower channels, such as Nares Strait and the QEI, passive microwave products are too coarse, so we rely on previously published values of ice flux that utilize higher resolution ice drift data. Total ice export into Nares Strait was determined from 1998-2009 by Kwok et al., (2010), while Howell et al., (2023) determined total and MYI flux into Nares Strait from 2017-2021. To estimate MYI flux prior to 2017 we first estimate total ice flux using the relationship that Kwok et al (2010) found between the duration of the period when ice drift was unobstructed by ice arches and total ice export. This relationship is approximated to be $F = 285.74 * duration - 19{,}577$, where duration is the number of days during each ice season (September minimum to September minimum) when the arch was not in place. To determine duration we use the timing of ice arch formation and collapse presented by Vincent et al., (2019) for 1979-2019, while for 2020 and 2021 we use the dates of formation presented by Kirillov et al., (2021) and estimate the date of breakup from daily MODIS imagery. The record of total ice flux into Nares Strait is presented in Figure S2. Finally, we estimate MYI flux from total ice flux by assuming a MYI proportion of 88%, which is based on the data presented by Howell et al., (2023).

Total ice export into the QEI has been quantified for the period from 1997-2002 (Kwok, 2006), 1997-2018 (Howell and Brady, 2019) and more recently 2017-2021 (Howell et al., 2023). MYI flux was also determined during the latter period and revealed that MYI comprises 85% of the total ice flux into the QEI. To build a record of MYI flux into the QEI, we use the values of total ice export from Howell and Brady (2019) for the period 1997-2016, and the average export of 8,000 km^2 from Kwok, (2006) for the period 1979-1996, then scale them by 85%.

MYI flux through Amundsen Gulf and M'Clure Strait are not considered in this budget. Amundsen Gulf is predominantly covered by seasonal ice and is therefore neither a source or sink of MYI (Babb et al., 2022). M'Clure Strait contains a mix of seasonal and MYI, but recent observations show that the oscillation between export and import averages out to a net seasonal ice flux of only 2 km^2 (Howell et al., 2023).

Collectively, the terms of MYI export, melt, and replenishment dictate the annual MYI budget (Figure 1B). The budget is summed for the annual ice season, which begins with replenishment after the minimum and runs to the following minimum, providing a net change in MYI area for each year.

Regional boundaries as defined by the NSIDC MASIE (Multisensor Analyzed Sea Ice Extent) mask (Figure 2) were used to quantify MYI transport between regions within the Arctic Ocean and to breakdown replenishment by region.

3.3 Ancillary Data

Monthly mean fields of 2 m air temperature (T) were retrieved from the ERA-5 reanalysis (Hersbach et al., 2020) and used to calculate the cumulative FDD (T < -1.8°C) from October to May, and MDD (T > 0°C) from June to September. MDD was tested for a correlation with MYI melt, while following Kwok (2007), the combination of FDD and MDD were tested for correlation with MYI replenishment.

4. Results and Discussion:

4.1 MYI Area

Over the 43-year study period, the annual MYI minimum and maximum areas declined significantly (p < 0.05) at -72,500 km^2 yr^{-1} and -61,000 km^2 yr^{-1}, respectively (Figure 2A). The minimum MYI area declined at a higher rate than the decline in minimum total sea ice area within the Arctic Ocean (-59,000 km^2 yr^{-1}), indicating MYI is being lost at a greater rate than FYI. However, the reduction in the minimum MYI area has not occurred linearly but rather through two stepwise reductions that interrupt three periods of relative stability in MYI area. The first stepwise reduction occurred between September 1988 and 1989, and coincides with the "flushing" of MYI through Fram Strait (Pfirman et al., 2004). The second stepwise reduction occurred between September 2005 and 2008, which is

known to be a period of increased MYI loss (Kwok, 2009) that is thought to have been conditioned by the first reduction in 1989 (Lindsay et al., 2009) and corresponds to a shift towards thinner ice across the Arctic Ocean (Sumata et al., 2023). The average minimum MYI area during these periods fell from 3.56±0.14 x 10^6 km^2 between 1980 and 1988, to 2.7±0.23 x 10^6 km^2 between 1989 and 2005, and finally 1.2±0.20 x 10^6 km^2 between 2008 and 2021. The minima during the three periods have statistically different means (p < 0.01).

The reduction in MYI area between the three periods was accompanied by a change in the spatial distribution of MYI in the Arctic Ocean with a retreat of the MYI edge towards the northern coast of Greenland and the CAA (Figure 2B). From 1980 to 1988 MYI covered much of the Arctic Ocean, with older ice types being advected through the Beaufort Gyre and remnant FYI being confined to the perimeter of the summer ice edge. From 1989 to 2005, a wide band of the oldest MYI was present along the coasts of the CAA and Greenland, stretching from the Beaufort Sea to Fram Strait, while FYI remained intact in the central Arctic and spanned across the eastern face of the ice pack. Following the collapse of MYI between 2006 and 2008, MYI coverage between 2008 and 2021 was dramatically altered compared to the previous periods. The oldest MYI types were typically only present immediately along the CAA with a portion extending into the Beaufort Sea and none of the oldest ice reaching Fram Strait. Furthermore, the reduction in MYI area coincides with an increase in ice drift speeds during each period (Figure 2B) as a younger ice pack is mechanically weaker and therefore more mobile (Kwok et al., 2013; Rampal et al., 2009).

The reduction in MYI area has been compounded by a dramatic loss of older MYI types (Figure 2). During the annual minimum, the area of MYI three years and older decreased 81% from 3.06 x 10^6 km^2 in the first period to 0.59 x 10^6 km^2 in the third period. The reduction is even more dramatic for MYI 5+ years old, which decreased 92% from 2.08 x 10^6 km^2 in the first period to 0.17 x 10^6 km^2 in the third period, and is likely even lower given that MYI area is skewed towards older ice types in the Ice Age dataset. Over the 43-year study period there are significant (p < 0.01) negative trends in the area of MYI 3 (-7,800 km^2 yr^{-1}), 4 (-9,400 km^2 yr^{-1}) and 5+ (-59,000 km^2 yr^{-1}) years old, but interestingly there is no trend in second year ice area, which has remained stable around its mean minimum of 0.65 x 10^6 km^2 but now comprises a greater proportion of the MYI pack.

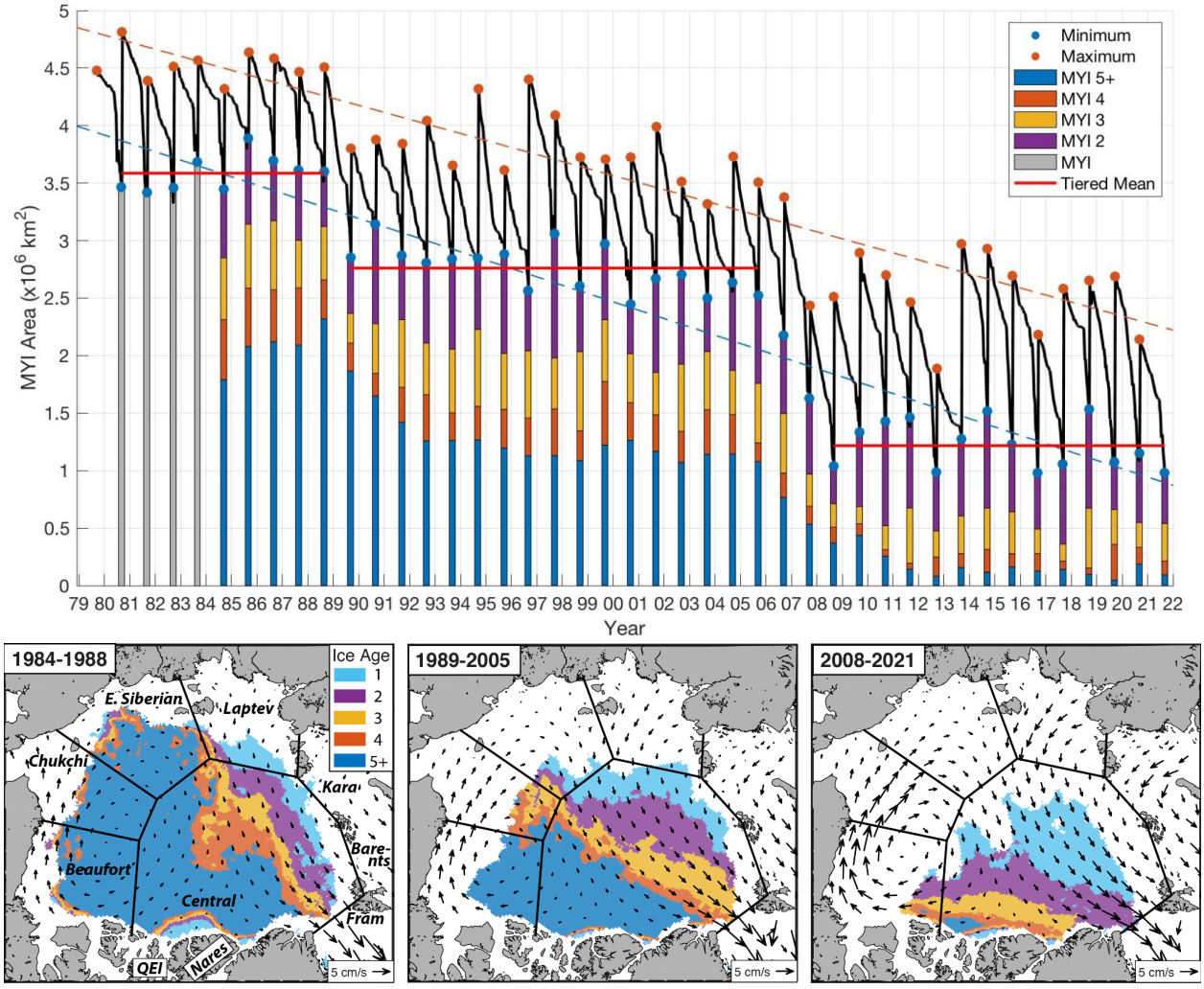

Figure 2: Top: Time series of the weekly MYI area in the Arctic Ocean beginning the week after the minimum of 1979 and running to the minimum of 2021. The MYI age distribution during the September minimum is presented by coloured bars for 1984 to 2021. Dots denote the MYI area during the minimum and maximum, with associated trend lines shown by dashed lines. The mean MYI minimum during the three periods are overlaid. Bottom: Maps of the median ice age during the minima of each period. The mean annual fields of ice drift are overlaid and the regional boundaries are also presented.

4.2: MYI Budget

To examine MYI loss during these two stepwise reductions and the equilibrium in MYI area that has existed during the three periods they separate, we now analyze the three terms and net annual balance of the MYI Budget.

4.2.1: MYI Export

On average 709,000 km^2 of MYI was exported from the Arctic Ocean annually over the record (Figure 3). A vast majority (648,300 km^2; 93%) of the export was through Fram Strait (Figure 3B) while the remaining 7% represents the balance of (i) export into Nares Strait and the QEI and (ii) transport (either import or export) across the boundaries to the Barents and Kara Seas.

MYI export from the Arctic peaked at 1.4 x 10^6 km^2 in 1995 (Figure 3). This agrees with the observed peak in total ice export through Fram Strait presented by Kwok (2009), which the authors attributed to an increased sea level pressure gradient across the strait that enhanced ice drift speeds. Total MYI export has only surpassed 1 x 10^6 km^2 two other times, 1989 and 2007, both of which contributed to the two stepwise reductions. In 1989, a record amount of the oldest MYI (MYI 5+; 634,000 km^2) was exported through Fram Strait after it had been flushed out of the Beaufort Gyre by a change in the AO (Figure 3; Pfirman et al., 2004). In 2007 a strong Transpolar Drift Stream increased ice export through Fram Strait (Nghiem et al., 2007), while anomalous ice export into Nares Strait (Kwok et al., 2010) compounded the total MYI export (Figure 3). For comparison, the minimum MYI export through Fram Strait occurred in 2018 (340,000 km^2) which coincides with an anomalous drop in sea ice volume export (Sumata et al., 2022).

Following the second stepwise reduction from 2006-2008, the age distribution of MYI being exported through Fram Strait was much younger, with the proportion of MYI 4+ years declining from 57% of the ice pack prior to 2007 to only 15% after 2007 (Figure 3B). Additionally, since 2007 both MYI and total ice export through Fram Strait declined significantly ($p < 0.05$) with respective rates of -19,600 and -15,900 km^2 yr^{-1} (Figure 3B). The discrepancy in these rates has reduced the MYI proportion of the total ice export through Fram Strait, which declined significantly ($p < 0.01$) at -6% per decade. Overall ice export through Fram Strait has shifted to more FYI and younger MYI, a change which is due to younger ice within the Transpolar Drift Stream (Figure 2; Comiso, 2012; Haas et al., 2008; Krumpen et al., 2019), and has undoubtedly contributed to the long-term reduction in sea ice volume export through Fram Strait (Kwok, 2009; Sumata et al., 2022).

Decreasing MYI export through Fram Strait has been partially offset by increasing MYI export into Nares Strait and the QEI, though the magnitudes of these increases are substantially lower than the trend in Fram Strait (Figure 3A). Historically, a small amount

of MYI was imported into the Arctic Ocean from the Kara Sea, however this source of MYI has been null since 2007 (Figure 3A). MYI export into the Barents Sea peaked at 160,000 km^2 in 2003, which corresponds to the peak observed by Kwok et al., (2005), but has a long term mean of only 12,900 km^2 yr^{-1} with no long term trend. Following the second stepwise reduction, MYI export into the Barents Sea has been null during half of the years.

Overall, following the second stepwise reduction a significant ($p < 0.05$) negative trend in MYI export through Fram Strait has been slightly offset by increasing MYI export into Nares Strait and the QEI, but overall the net annual MYI export from the Arctic has decreased at a rate of 19,200 km^2 yr^{-1} (Figure 3B). While on average 93% of the MYI export was through Fram Strait, this proportion declined from 95% prior to 2007 to 87% since 2007, as the consolidation of MYI in the central Arctic and decreases in ice arch duration within Nares Strait and the QEI (Moore et al., 2021; Howell and Brady, 2019) has altered the balance of MYI export.

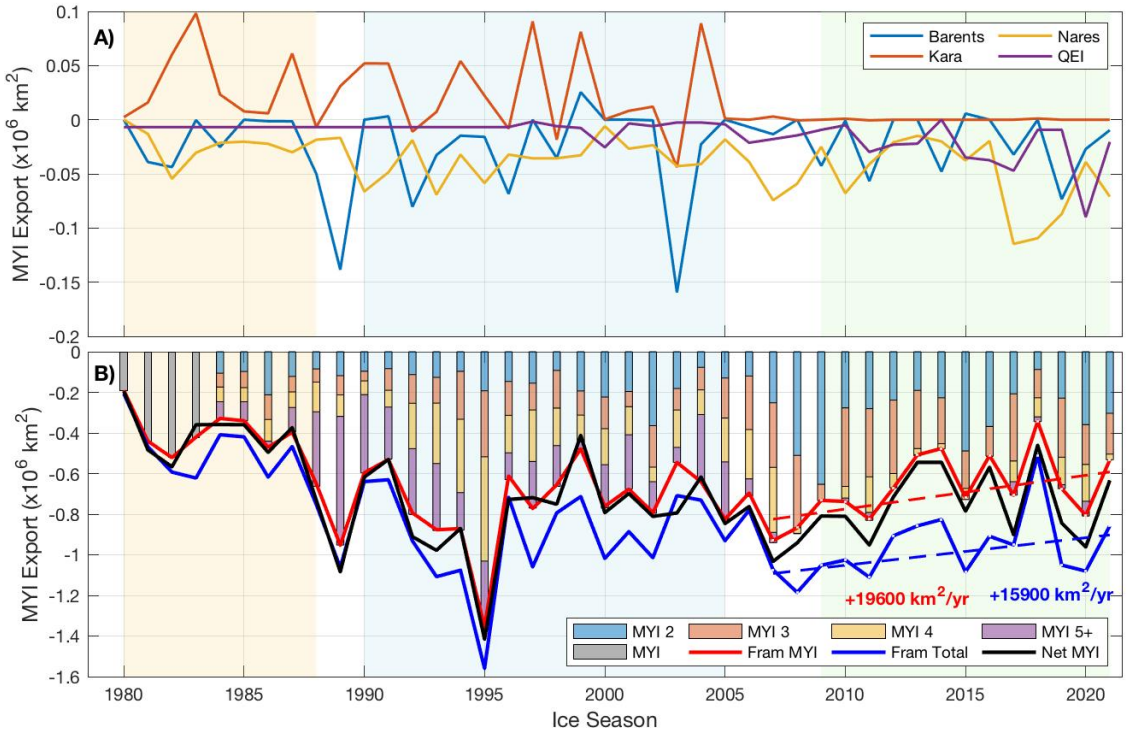

Figure 3: Annual record of MYI export across the boundaries of the Arctic Ocean from the ice season of 1980 to 2021. (top) MYI transport into Nares Strait and the QEI, Barents Sea and Kara Sea. (bottom) MYI and total ice transport through Fram Strait, along with the net MYI export for each year and the MYI age distribution of MYI export through Fram Strait (bars).

Positive values indicate import, while negative values indicate export. Significant trends are presented with dashed lines.

4.2.2: MYI Melt

Across the Arctic Ocean, an average of 481,000 km^2 of MYI was lost to melt annually between 1980 and 2021 (Figure 4). MYI melt peaked at 1.15 x 10^6 km^2 in 2016 and was near 0 km^2 in 1994. There is no significant trend over the full 43-year record, though there is a significant (p < 0.01) negative trend of ~17,200 km^2 yr^{-1} since the first stepwise reduction. Based on the results of Babb et al., (2022), approximately one-third of this increase has occurred in the Beaufort Sea, where MYI melt increased at a rate of 6,000 km^2 yr^{-1} between 1997 and 2021, causing MYI transport through the Beaufort Gyre to be interrupted. Coincident to the increase in MYI melt has been a significant increase in MDD over the Arctic Ocean of 2 degree-days yr^{-1}, i.e. 82 degree-days total over the study period (Figure 5). MYI melt and MDD are significantly correlated (r = 0.38, p < 0.01) with melt increasing by 3,300 km^2 for every additional degree-day increase in MDD.

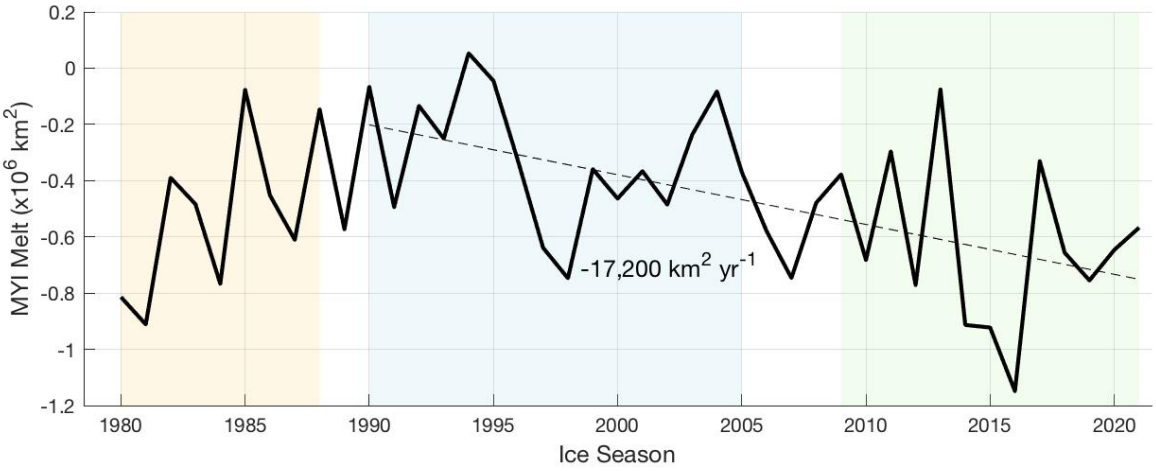

Figure 4: Annual area of MYI melt for the Arctic Ocean. The dashed line shows the negative trend from 1990 to 2021. The significant trend is presented as a dashed line.

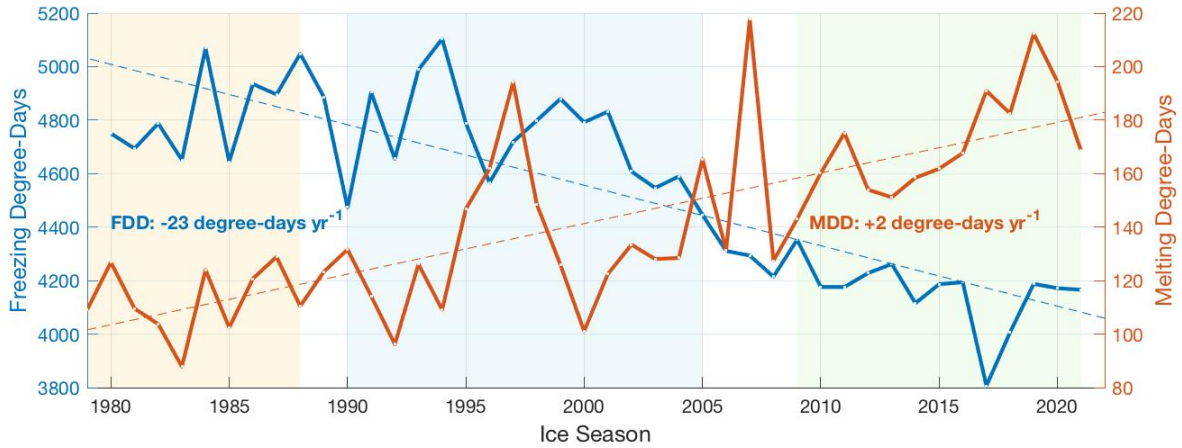

Figure 5: Time series of the spatially averaged FDD and MDD over the Arctic Ocean from October to May and June to September, respectively. Significant trends are presented by dashed lines.

4.2.3: MYI Replenishment and Retention

MYI replenishment is the largest term in the MYI budget, averaging 1.11 x 10^6 km^2 per year (Figure 6A). However as the sole source of MYI it must offset export and melt if the MYI budget is to balance annually. Over the study period MYI replenishment significantly ($p < 0.05$) increased at a rate of +11,000 km^2 yr^{-1}. The peak in MYI replenishment occurred in 1996 (1.8 x 10^6 km^2), yet the next six largest years of replenishment have all occurred since 2005. The minimum replenishment occurred in 1987 (700,000 km^2) and may have helped to condition the first stepwise reduction in 1989, while the largest negative anomalies relative to the positive trend occurred during years of record sea ice minima (1998, 2007 and 2012) and coincide with increased melt (Figure 4) during particularly warm years (Figure 5). However, over the study period replenishment and melt from the same year are not correlated, meaning increased MYI melt does not correspond to increased FYI melt and thereby reduced MYI replenishment. Although replenishment and melt are not correlated for the same summer, replenishment is negatively correlated ($r = 0.46$, $p < 0.01$) with melt during the following summer. This relationship is important; increasing replenishment creates a thinner MYI pack during the following melt season, increasing the area of MYI that melts.

Our values of MYI replenishment are significantly higher than those previously presented by Kwok (2004; 2007) and Kwok et al., (2009). Particularly in 2005 and 2007

when those studies showed near-zero replenishment (<0.1 x 10^6 km^2) and we calculated replenishment of 0.93 x 10^6 km^2 and 0.83 x 10^6 km^2, respectively. The reason for this discrepancy is the different methods used to calculate replenishment. We calculate the area of second year ice one week after the minimum from the Ice Age dataset, which accounts for the reduction in MYI area not just through export but also through melt. The method developed by Kwok (2004) only accounts for MYI export through Fram Strait and assumes that no MYI is lost to melt. As a result their method overestimated the MYI area in September, which led to an underestimate of MYI replenishment. Our method also underestimates replenishment as surviving FYI within MYI pixels is not accounted for.

Replenishment primarily occurs along the fringe of the summer ice pack where FYI buttresses up against the MYI pack, though a portion does occur within the MYI pack in areas of divergence where FYI has formed (Figure 7). Historically, replenishment was approximately split evenly between the marginal seas and the central Arctic (Figure 6B). That changed during the second stepwise reduction as the summer ice edge retreated north of the regional boundaries and reduced the survival of FYI in the marginal seas. Concurrently, the consolidation of the MYI edge exposed a greater area of the central Arctic to FYI that - protected by colder temperatures at northern latitudes- could persist through the melt season (Figure 7E). As a result, since 2007 MYI replenishment in the Chukchi, East Siberian and Laptev Seas has decreased by over 50% while MYI replenishment in the central Arctic has doubled. Meanwhile, there has been no change in MYI replenishment in the Beaufort Sea despite an increase in FYI area during winter (Galley et al., 2016). The fact that increasing FYI area during winter has not translated to an increase in MYI replenishment indicates that FYI in the Beaufort Sea is typically not thick enough to survive through the melt season and replenish the MYI pack (i.e. Galley et al., 2013), and further highlights the regional variability and importance of latitude for replenishment. Examining the distribution of replenishment area by latitude during the three periods of MYI stability, we find a clear northward transition over time that coincides with the poleward decrease in air temperatures during the melt season (May to September; Figure 7E). The dramatic reduction in replenishment in the marginal seas has transitioned replenishment from a bimodal distribution with peaks at ~72N and ~82°N to a unimodal distribution around a peak at ~83°N with very little replenishment occuring south of 75°N since 2008.

570 Warming between the three periods is also evident, with an increase of ~2°C at
571 70°N and ~0.5°C at the pole (Figure 7E). Significant ($p < 0.05$) trends towards fewer FDD (-
572 23 degree-days yr^{-1}) and more MDD (+2 degree-days yr^{-1}; Figure 5) would intuitively
573 reduce MYI replenishment as there is less FYI growth during winter and more FYI melt
574 during summer. However, we find a clear increase in MYI replenishment that shows no
575 relationship with pan-Arctic MDD and surprisingly a significant inverse relationship with
576 pan-Arctic FDD ($r = -0.45$, $p < 0.01$) that indicates other factors must be driving the
577 observed increase in replenishment. Based on the regional changes in MYI replenishment it
578 is clear that the increase has primarily been driven by the northward migration of FYI into
579 the central Arctic where it is subject to cooler temperatures and less incident solar
580 radiation facilitating less melt. To support this we find that the area of both FYI and MYI at
581 the end of winter (the last week of April) are significantly ($p < 0.01$) correlated with MYI
582 replenishment. FYI area has a positive relationship ($r = 0.61$) while MYI area has a negative
583 relationship ($r = -0.61$) implying that more FYI and less MYI at the start of the melt season
584 leads to more MYI replenishment. This highlights a negative feedback in the Arctic system
585 that stabilizes the MYI area by compensating for MYI loss through increased MYI
586 replenishment. However, this MYI feedback requires that FYI grow thick enough during
587 winter to survive the melt season, which is part of the negative conductive feedback (Bitz &
588 Roe, 2004). There is already evidence that the current level of warming has weakened the
589 negative conductive feedback (Ricker et al., 2021; Stroeve et al., 2018) and projections that
590 it will eventually be overwhelmed by warming (Petty et al., 2018). Yet in the near term, the
591 MYI feedback may continue to provide some stability to the MYI pack.
592 A limitation to the stability that results from the MYI feedback is that MYI
593 replenishment only reflects the retention of FYI into second year ice, while MYI of all ages
594 are lost to export and melt. This imbalance highlights an underlying transition in the MYI
595 pack towards younger and therefore thinner MYI that is undercutting the stability that the
596 positive trend in replenishment is facilitating. Hence, the continued retention of sea ice into
597 progressively older and thicker MYI is key to maintaining the MYI pack. Over the 43 year
598 study period the retention of second year ice significantly increased and the retention of
599 MYI 3 years old was fairly stable, while retention of MYI 4 and 5+ years old significantly
600 declined (Figure 6C). The reduced retention to older MYI types is primarily due to the

increase in MYI melt in the Beaufort Sea (Babb et al., 2022) which has interrupted MYI transport through the Beaufort Gyre and therefore precludes ice from aging while being retained within the Gyre. As it is now, MYI is only able to age for as long as it can remain in the Central Arctic before it is either siphoned off into the Beaufort Sea, exported into Nares Strait or the QEI, or advected towards Fram Strait.

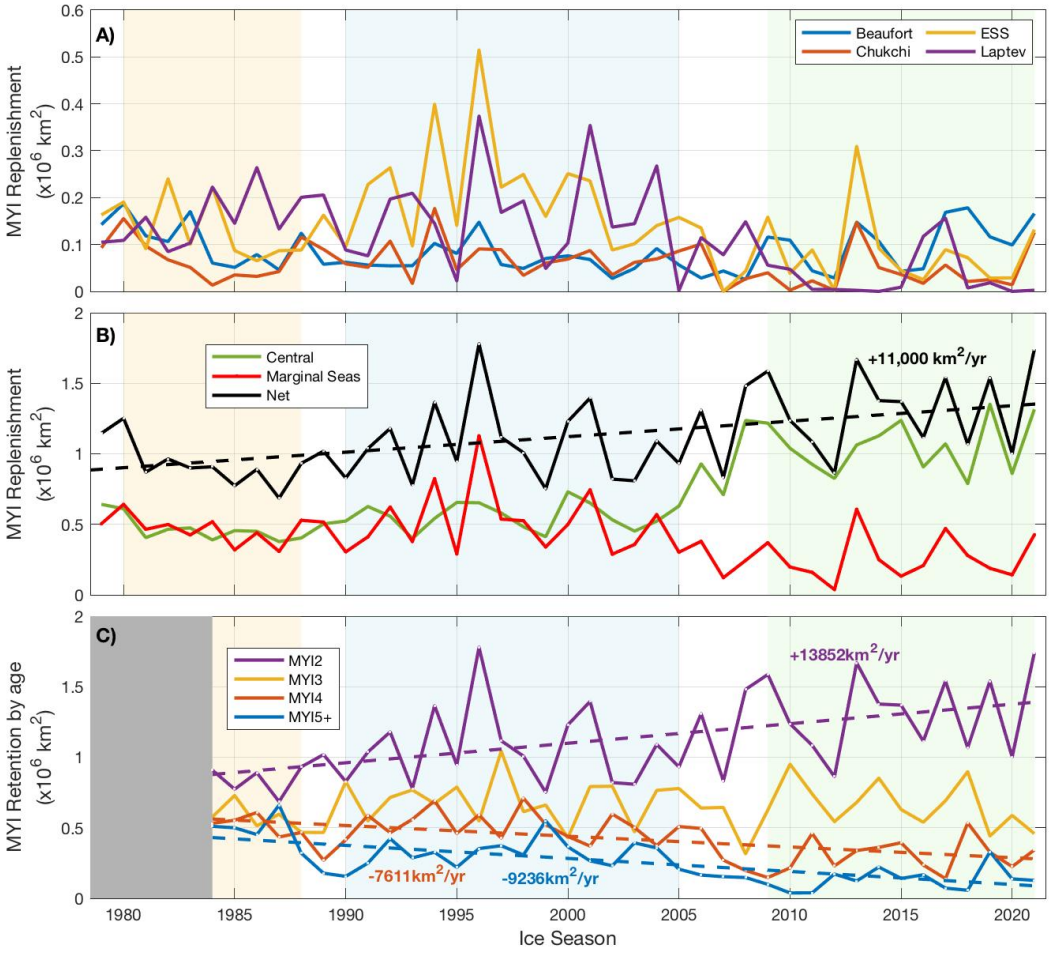

Figure 6: Annual area of MYI replenishment for A) each of the marginal seas and B) the central Arctic and sum of the marginal seas for the total MYI replenishment. C) MYI retention by age. Note that retention of MYI 2, 3 and 4 are calculated as their area during the week after the minimum, while MYI5+ is calculated as the change in MYI5+ area from them minimum to the week after, representing the increase in area of MYI 5+ and therefore the retention of that age of ice. Significant trends are presented with dashed lines.

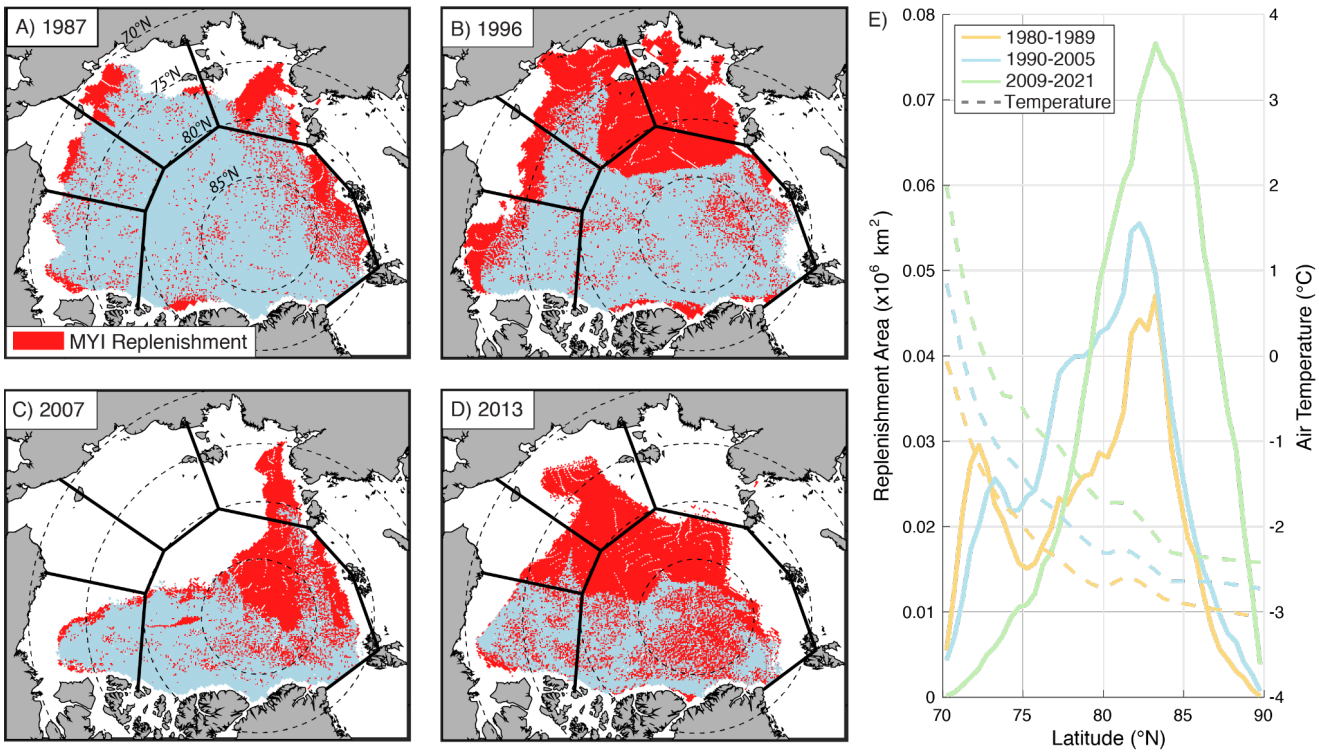

Figure 7: Areas of MYI replenishment during A) 1987, B) 1996, C) 2007 and D) 2013. Areas of MYI replenishment are presented in red, while the rest of the ice pack is presented in light blue. Regional boundaries are overlaid in black. E) Latitudinal distributions of replenishment area (solid lines) and mean air temperature during the melt season (May to SEptember; dashed lines) for the three stable periods of MYI. Note that latitudinal distributions are based solely on data within the boundaries of the Arctic Ocean.

4.2.4: MYI Budget of the Arctic Ocean.

With each of the three MYI terms calculated, we now close the annual MYI budget of the Arctic Ocean for the ice seasons from 1980 to 2021 and determine the net balance for each year (Figure 8A). The net balance shows very close agreement with the change in MYI area calculated from one minimum to the next, indicating our budget captures the vast majority of the changes in MYI area within the Arctic Ocean (Figure 8B). The average annual terms of the MYI budget are; i) Export: -709,000 km^2, ii) Melt: -463,000 km^2 and iii) Replenishment: 1,106,000 km^2, for an average annual loss of 65,000 km^2 yr^{-1} over the 43 year study period. However, there is considerable variability between years of MYI loss and MYI gain. The greatest MYI loss occurred in 1989 (-719,000 km^2), driving the first stepwise reduction in MYI area. The record loss in 1989 was the result of positive anomalies in export (+56%; +387,140 km^2) and melt (+19%; +92,450 km^2) coupled with a negative

anomaly in replenishment (-16%; -174,590 km^2). Conversely, the highest MYI gain occurred in 2018 (490,000 km^2), due to a negative anomaly in export (-43%; -295,870 km^2) and positive anomaly in replenishment (+39%; +434,200 km^2), and despite a positive anomaly in melt (+36%; +175,180 km^2). Contrasting between years of MYI loss and gain against the mean magnitude of each term, reveals that a net loss corresponds to greater export (+57,000 km^2) and melt (+26,000 km^2) and much less replenishment (-95,000 km^2), while a net gain corresponds to reduced export (-93,000 km^2) and melt (-42,000 km^2) and much more replenishment (+155,000 km^2). While all three terms contribute to the direction of the net balance, replenishment has the greatest magnitude and even exceeds the combined anomaly of export and melt during years with a net gain or net loss, hence replenishment has the greatest influence on the overall net MYI balance.

Beyond the MYI balance of an individual year, it is important to look at the balance over a few years as individual years of MYI loss or gain can often be offset by a contrasting swing in subsequent years that can either stabilize the MYI pack or dramatically (and permanently) change it. For example between 1995 and 2001 the MYI budget oscillated between large losses and gains, with the peak export (1995) and replenishment terms (1996) terms occurring during this period, but overall they offset each other and the MYI area remained relatively stable through this time (Figure 8). Similarly, the loss of MYI in 2012, which was primarily due to anomalously high melt (+60%; 290,870 km^2), was immediately offset by MYI gains in 2013 and 2014. This recovery was the result of cooler temperatures and a consolidated ice pack through the 2013 melt season (Kwok, 2015; Tilling et al., 2015) which reduced melt in 2013 (-84%; -405,550 km^2) and led to record replenishment in 2014 (+51%; +562,690 km^2; occurring during fall 2013). However, losses are not always offset in subsequent years. For example, the second stepwise reduction in MYI area occurred between 2006 and 2008 when approximately 1.4 x 10^6 km^2 of MYI was lost, which is slightly less than the MYI area loss of 1.54 x 10^6 km^2 reported by Kwok et al. (2009). Focusing on this period of MYI loss we find that 2006 was characterized by increased melt (+21%; +99,000 km^2) and reduced replenishment (-16%; -174,850 km^2) with near average export (+9%; +58,821 km^2). 2007 was characterized by increased export (+45%; +312,930 km^2) and melt (+55%; +265,700 km^2), and actually experienced increased replenishment relative to the long term mean (+18%; +201,890 km^2; opposite to

665 what Kwok et al., (2009) showed). 2008 had the second greatest annual loss of MYI on
666 record and was primarily the result of increased export (+33%; +227,950 km^2) and
667 reduced replenishment (-25%; -275,400 km^2; from autumn 2007) with near-average melt
668 (0%). Clearly it was not just one term that facilitated the second stepwise reduction in MYI
669 area but rather anomalous export, melt and replenishment over consecutive years steadily
670 compounding the overall decline and driving a significant change in the MYI pack.

671 During the three periods of stability in the minimum MYI area, melt and export were
672 in equilibrium with replenishment (Figure 8B). However, the proportion of export and melt
673 changed between periods. During the first period export and melt were similar in
674 magnitude, whereas during the second period export was more than twice as great as melt.
675 During the third period, the two returned to being approximately equal in magnitude,
676 cleanly breaking the budget down between approximately one-quarter melt, one-quarter
677 export and one-half replenishment. With trends towards declining export and increasing
678 melt, the role of each term in the MYI budget is likely to continue swinging towards MYI
679 melt exceeding MYI export. For reference, MYI melt exceeded MYI export during only nine
680 of the 43 years analyzed here, though five of these have occurred since 2010, highlighting
681 the increasing role of MYI melt in the MYI budget of the Arctic Ocean.

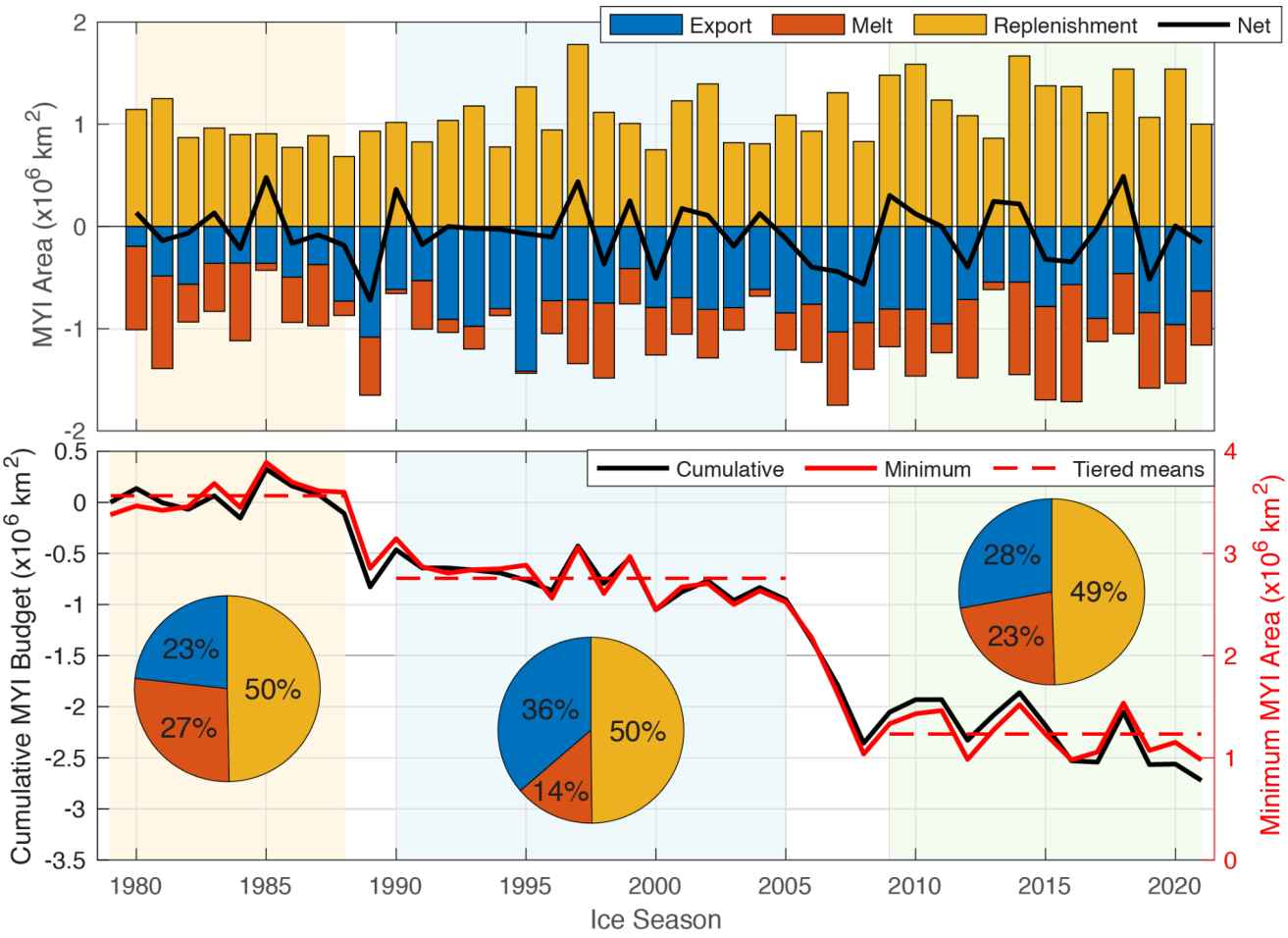

Figure 8: Top: Stacked bar plots of the annual MYI budget with the net overall results presented in black. Bottom: Time series of the cumulative annual result of the MYI budget (blue) and the MYI area minimum (red). Pie charts of the average contribution of each term to the overall budget are presented for each of the three periods. The three periods of MYI stability are highlighted by shading.

4.3 The Future of MYI

The Arctic is projected to be seasonally ice-free (<1 x 10^6 km^2) as soon as the 2030s or 2050s (Kim et al., 2023; SIMIP Community, 2020), at which point the Arctic Ocean will only be seasonally covered by FYI while a small area of MYI will be confined to the northern regions of CAA and Greenland known as the Last Ice Area. The projected near-complete loss of MYI in the not-too distant future indicates the MYI budget of the Arctic Ocean will continue to be in a deficit. Based on our results, we can expect that future MYI loss will likely occur through a series of stepwise reductions with periods of relative

699 stability in between. Using the MYI budget we speculate on the contribution of each term to
700 the future loss of MYI.

701 First, it is worth noting that any appreciable recovery of MYI is highly unlikely in the
702 foreseeable future as that would require several years of reduced MYI loss (export and
703 melt) coupled with increased replenishment and further retention of MYI into older and
704 thicker MYI. Individual years of recovery do continue to occur (i.e. 2013 and 2018; Figure
705 8) and maintain the current state of equilibrium, yet a stepwise increase in MYI area would
706 require several consecutive years with a net gain in MYI area and most importantly
707 retention into older MYI that is thicker and therefore more resilient against melt. This has
708 not happened at any point over the satellite era.

709 Export drove the first stepwise reduction in 1989 and contributed to the second
710 reduction between 2006 and 2008. However, the consolidation of the MYI pack away from
711 the area upstream of Fram Strait has led to a negative trend in MYI export since 2008 that
712 has reduced the overall impact of export on the MYI budget and leads us to suggest that
713 export will not be a main driver of future MYI loss. Instead, we speculate that the future
714 loss of MYI will be driven by the combination of high melt and low replenishment,
715 reinforced over several consecutive years. Given that these two terms are related to ice
716 melt, it is intuitive that a particularly warm summer would increase both FYI and MYI melt,
717 with the former limiting replenishment. Conditioning during the preceding winter is also
718 critical to these terms as a strong Beaufort Gyre would expose more MYI to increased melt
719 rates in the Beaufort Sea (i.e. 2021; Babb et al., 2022; Mallett et al., 2021) while a warm
720 winter would limit FYI growth and therefore replenishment (i.e. 2015; Ricker et al., 2017).
721 Considerable MYI replenishment is already occurring in the Central Arctic (Figure 7),
722 where surface air temperatures in the Arctic are coldest, enabling a long-term positive
723 trend in replenishment. However, with further reductions in September sea ice extent the
724 area available for FYI to survive and replenish MYI will dwindle, causing the positive trend
725 in replenishment to level off and eventually decline.

726 MYI area melt is likely to continue increasing in the coming years as air
727 temperatures increase (greater MDD, lower FDD), while a transition of the MYI pack itself
728 towards younger thinner MYI makes it less resilient and more susceptible to melt. The
729 transition to younger ice types is being driven by an imbalance between ice of all ages

being lost to export and melt, whereas only the replenishment of second year ice is increasing in contrast to reduced retention of older MYI ages. As a result the MYI cover continues to thin (Kacimi & Kwok, 2022; Krishfield et al., 2014; Kwok & Rothrock, 2009; Petty et al., 2023), making it more mobile and facilitating the formation of large polynyas within the Last Ice Area during recent years (Moore, Howell, & Brady, 2021; Schweiger et al., 2021). As a result, Schweiger et al., (2021) suggest that the remaining MYI pack is proving to be less resilient to warming than previously expected.

Ultimately we speculate that the future loss of MYI is likely to be driven by gradually increasing melt and reduced replenishment, but conditioned by the transition towards a younger thinner MYI pack. With each reduction, the MYI pack will retreat even further towards the Last Ice Area along the coast of the CAA. Eventually the Arctic Ocean is projected to become seasonally ice-free, at which time the remaining MYI will be confined to the narrow channels of the CAA and there will be no replenishment within the Arctic Ocean.

5: Conclusions

The loss of MYI and transition to a predominantly seasonal ice cover in the Arctic Ocean has been one of the greatest changes taking place in the Arctic. Using a 43 year dataset on sea ice age, we have examined the loss of MYI area and the relative contribution of melt, export and replenishment to this loss. Overall, MYI area during the annual September sea ice minimum has significantly declined at a rate of -72,500 km^2 yr^{-1}; however, MYI loss has not occurred continuously but rather through two stepwise reductions that separated three prolonged periods of relative stability. During these stable periods, MYI loss through export and melt was wholly offset by replenishment, maintaining equilibrium within the MYI pack. Conversely during the two stepwise reductions MYI loss greatly exceeded replenishment, driving a dramatic reduction in MYI area and a concurrent northward contraction of the MYI pack towards the coast of the CAA. The first reduction occurred in 1989 after a change in the AO flushed MYI out of the Beaufort Gyre into the Transpolar Drift Stream and subsequently led to anomalously high MYI export through Fram Strait, with a peak in the export of the oldest MYI types. The second reduction occurred between 2006 and 2008 and was the result of anomalously high melt and export,

761 coupled with anomalously low replenishment. The consolidation of the MYI pack during
762 the second reduction reduced the presence of MYI upstream of Fram Strait, leading to a
763 significant decline in MYI export and transition towards younger ice being exported
764 through Fram Strait. At the same time, MYI export into Nares Strait and the QEI has
765 increased, albeit at a much smaller magnitude, however, MYI export through these
766 pathways is important because it is the oldest MYI that is lost.

767 While there is no long term trend in MYI export, MYI melt has significantly increased
768 since 1989 while MYI replenishment has significantly increased over the full 43-year study
769 period. The trend in MYI melt is the result of warming temperatures and a transition to
770 younger and thinner MYI that is less resilient to warmer temperatures and the associated
771 ice-albedo feedback. MYI area melt is found to be correlated with MDD and increases 3,300
772 km^2 for every additional degree-day above 0°C. The trend in replenishment is not
773 correlated with MDD, even though replenishment should reflect FYI melt, or FDD, which
774 reflects FYI growth during the preceding winter. Instead, we suggest that the increase in
775 replenishment has been driven by the northward contraction of the MYI edge which in turn
776 provides greater space for FYI to survive through the melt season at higher latitudes;
777 highlighting a negative feedback that serves to stabilize the MYI pack. While the increase in
778 replenishment has dampened MYI loss and fostered three periods of stability, there is an
779 underlying transition towards younger MYI as the retention of MYI to older ice types has
780 declined. This is a change dominated by increasing melt in the Beaufort Sea interrupting
781 the transport of MYI through the Beaufort Gyre which precludes the ice from aging as it had
782 historically. Additionally, replenishment is found to be correlated with melt during the
783 following summer, meaning that increased replenishment promotes a younger thinner MYI
784 pack that is more susceptible to melt.

785 Overall, the MYI pack has been stable around a minimum area of 1.2×10^6 km^2 since
786 2008. However, this stability has been undercut by the continued transition to younger and
787 thinner MYI, with the recent occurrence of large polynyas within the MYI pack suggesting it
788 is not as resilient as previously expected and may be poised for another stepwise
789 reduction. Eventually the Arctic is projected to be seasonally ice-free, at which point MYI
790 will be confined to the narrow channels of the CAA. In the meantime we expect MYI loss to
791 continue to occur episodically rather than continuously. The two previous stepwise

792 changes reduced Arctic MYI area by 0.9 and 1.5 x 10^6 km^2, meaning that a future reduction
793 of similar magnitude would render the Arctic Ocean essentially MYI free. Based on the
794 budget we do not expect MYI to recover and we expect future loss to mainly be driven by
795 the combination of increased melt and reduced replenishment. Both of these mechanisms
796 are promoted by warming trends during summer and conditioned by a combination of MYI
797 transport and FYI growth during the preceding winter. Ultimately, the MYI budget of the
798 Arctic Ocean reflects a balance of several factors that have generally been in equilibrium
799 through much of our 43 year study period. However, occasionally MYI loss has greatly
800 exceeded replenishment, leading to a dramatic reduction and, within the timescale of this
801 study, unrecoverable change in the MYI pack. While a negative feedback in MYI
802 replenishment has so far dampened MYI loss, continued warming that both increases MYI
803 melt and limits MYI replenishment will eventually lead to the complete loss of MYI and
804 transition to a seasonally ice-free Arctic Ocean.

Acknowledgements:

Tragically D. Barber passed away in the early stages of writing this paper; he was a giant in Arctic research and will be remembered as such. D. Babb, R. Galley, J. Ehn and D. Barber would like to acknowledge the financial support from the Natural Sciences and Engineering Research Council of Canada (NSERC). D. Babb and S. Kirillov were supported by the Canada Research Chair (CRC - D. Barber) and Canada Excellence Research Chair (CERC - D. Dahl-Jensen) programs. D. Babb acknowledges additional financial support from the Canadian Meteorological and Oceanographic Society (CMOS). J. Landy acknowledges support from the CIRFA project under Grant #237906 and the INTERAAC project under grant #328957 from the Research Council of Norway (RCN), and from the Fram Centre program for Sustainable Development of the Arctic Ocean (SUDARCO) under grant #2551323. J. Stroeve acknowledges support from the Canada 150 Chair Program. W. Meier acknowledges support from the NASA Cryospheric Sciences Program (Grant #80NSSC21K0763**).** We acknowledge the use of imagery from the NASA Worldview application (https://worldview.earthdata.nasa.gov), part of the NASA Earth Observing System Data and Information System (EOSDIS). Thanks to J.S. Stewart at NSIDC for help with the 1979-1983 ice age data. Thanks to M. Bushuk for helpful conversations during the development of this work.

Data Availability Statement:

Sea ice concentration, drift and age datasets are available from the National Snow and Ice Data Center (NASA-Team sea ice concentration - https://nsidc.org/data/NSIDC-0051/versions/1; Polar Pathfinder 25 km Drift v4 - https://nsidc.org/data/nsidc-0116/versions/4; EASE-Grid Sea Ice Age v4 - https://nsidc.org/data/NSIDC-0611/versions/4). The early EASE –Grid Sea Ice Age data from 1978-1983 is available through Zenodo (https://zenodo.org/record/7659077). ERA5 reanalysis products are available from the Climate Data Store through the Copernicus Climate Change Service (https://cds.climate.copernicus.eu/cdsapp#!/home).

References:

Babb, D. G., Galley, R. J., Asplin, M. G., Lukovich, J. V., & Barber, D. G. (2013). Multiyear sea ice export through the Bering Strait during winter 2011-2012. *J. Geophys. Res. Ocean.*, *118*(10), 5489–5503. https://doi.org/10.1002/jgrc.20383

Babb, D. G., Galley, R. J., Howell, S. E. L., Landy, J. C., Stroeve, J. C., & Barber, D. G. (2022). Increasing Multiyear Sea Ice Loss in the Beaufort Sea: A New Export Pathway for the Diminishing Multiyear Ice Cover of the Arctic Ocean. *Geophys. Res. Lett.*, *49*(9), 1–11. https://doi.org/10.1029/2021GL097595

Barber, D. G., Babb, D. G., Ehn, J. K., Chan, W., Matthes, L., Dalman, L. A., Campbell, Y., Harasyn, M. L., Firoozy, N., Thériault, N., Lukovich, J. V., Zagon, T., Papakyriakou, T., Capelle, D. W., Forest, A., & Gariepy, A. (2018). Increasing Mobility of High Arctic Sea Ice Increases Marine Hazards Off the East Coast of Newfoundland. *Geophys. Res. Lett.*, *45*(5), 2370–2379. https://doi.org/10.1002/2017GL076587

Bitz, C. M., & Roe, G. H. (2004). A mechanism for the high rate of sea ice thinning in the Arctic Ocean. *J. Clim.*, *17*(18), 3623–3632. https://doi.org/10.1175/1520-0442(2004)017<3623:AMFTHR>2.0.CO;2

Bourke, R. H., & Garret, R. P. (1987). Sea ice thickness distribution in the Arctic Ocean. *Cold Reg. Sci. Technol.*, *13*, 259–280.

Boutin, G., Ólason, E., Rampal, P., Regan, H., Lique, C., Talandier, C., Brodeau, L., & Ricker, R. (2023). Arctic sea ice mass balance in a new coupled ice-ocean model using a brittle rheology framework. *Cryosphere*, *17*(2), 617–638. https://doi.org/10.5194/tc-17-617-2023

Cavalieri, D. J., Parkinson, C. L., Gloersen, P., & Zwally, H. J. (1996). *Sea Ice Concentrations from Nimbus-7 SMMR and DMSP SSM/I-SSMIS PAssive Microwave Data*.

Comiso, J. C. (2012). Large decadal decline of the arctic multiyear ice cover. *J. Clim.*, *25*(4), 1176–1193. https://doi.org/10.1175/JCLI-D-11-00113.1

Constable, A. J., Harper, S., Dawson, J., Holsman, K., Mustonen, T., Piepenburg, D., & Rost, B. (2022). Cross Chapter Paper 6: Polar Regions. In H. O. Portner, D. C. Roberts, M. Tignour, E. S. Poloczanska, K. Mintenbeck, A. Alegria, M. Craig, S. Langsdorf, S. Loscke, V. Moller, A. Okem, & B. Rama (Eds.), *Climate Change 2022: Impacts, Adaptation and Vulnerability.* (pp. 2319–2368). Cambridge University Press. https://doi.org/10.1017/9781009325844.023

Galley, R. J., Babb, D. G., Ogi, M., Else, B. G. T., Geifus, N. X., Crabeck, O., Barber, D. G., & Rysgaard, S. (2016). Replacement of multiyear sea ice and changes in the open water season duration in the Beaufort Sea since 2004. *J. Geophys. Res. Ocean.*, *121*(April), 1–18. https://doi.org/10.1002/2015JC011583.Received

Galley, R. J., Else, B. G. T., Prinsenberg, S., Babb, D. G., & Barber, D. G. (2013). Sea ice concentration, extent, age, motion and thickness in regions of proposed offshore oil and gas development near the Mackenzie Delta-Canadian Beaufort Sea. *Arctic*, *66*(1), 105–116.

Gow, A. J., & Tucker, W. B. (1987). Physical properties of sea ice discharged from Fram Strait. *Science (80-.).*, *236*(4800), 436–439. https://doi.org/10.1126/science.236.4800.436

Haas, C., Pfaffling, A., Hendricks, S., Rabenstein, L., Etienne, J. L., & Rigor, I. G. (2008). Reduced ice thickness in Arctic Transpolar Drift favors rapid ice retreat. *Geophys. Res. Lett.*, *35*(17), 1–5. https://doi.org/10.1029/2008GL034457

Hansen, E., Gerland, S., Granskog, M. A., Pavlova, O., Renner, A. H. H., Haapala, J., Løyning, T. B., & Tschudi, M. A. (2013). Thinning of Arctic sea ice observed in Fram Strait: 1990-2011. *J. Geophys. Res. Ocean.*, *118*(10), 5202–5221. https://doi.org/10.1002/jgrc.20393

Hersbach, H., Bell, B., Berrisford, P., Hirahara, S., Horányi, A., Muñoz-Sabater, J., Nicolas, J., Peubey, C., Radu, R., Schepers, D., Simmons, A., Soci, C., Abdalla, S., Abellan, X., Balsamo, G., Bechtold, P., Biavati, G., Bidlot, J., Bonavita, M., … Thépaut, J.-N. (2020). The ERA5 global reanalysis. *Q. J. R. Meteorol. Soc.*, *146*(730), 1999–2049. https://doi.org/https://doi.org/10.1002/qj.3803

Hibler, W. D., Hutchings, J. K., & Ip, C. F. (2006). sea-ice arching and multiple flow States of Arctic pack ice. *Ann. Glaciol.*, *44*, 339–344. https://doi.org/10.3189/172756406781811448

Howell, S. E. L., Babb, D. G., Landy, J. C., & Brady, M. (2022). Multi-Year Sea Ice Conditions in the Northwest Passage: 1968–2020. *Atmosphere-Ocean*, 1–15. https://doi.org/10.1080/07055900.2022.2136061

Howell, S. E. L., Babb, D. G., Landy, J. C., Moore, G. W. K., Montpetit, B., & Brady, M. (2023). A Comparison of Arctic Ocean Sea Ice Export Between Nares Strait and the Canadian Arctic Archipelago. *J. Geophys. Res. Ocean.*, *128*(4). https://doi.org/10.1029/2023JC019687

Howell, S. E. L., & Brady, M. (2019). The Dynamic Response of Sea Ice to Warming in the Canadian Arctic Archipelago. *Geophys. Res. Lett.*, *46*(22), 13119–13125. https://doi.org/10.1029/2019GL085116

Jahn, A., Sterling, K., Holland, M. M., Kay, J. E., Maslanik, J. A., Bitz, C. M., Bailey, D. A., Stroeve, J., Hunke, E. C., Lipscomb, W. H., & Pollak, D. A. (2012). Late-twentieth-century simulation of arctic sea ice and ocean properties in the CCSM4. *J. Clim.*, *25*(5), 1431–1452. https://doi.org/10.1175/JCLI-D-11-00201.1

Kacimi, S., & Kwok, R. (2022). Arctic Snow Depth, Ice Thickness, and Volume From ICESat-2 and CryoSat-2: 2018–2021. *Geophys. Res. Lett.*, *49*(5), 2018–2021. https://doi.org/10.1029/2021gl097448

Kim, Y., Min, S., Gillett, N. P., Notz, D., & Malinina, E. (2023). Observationally-constrained projections of an ice-free Arctic even under a low emission scenario. *Nat. Commun.*, *14*(1), 3139. https://doi.org/10.1038/s41467-023-38511-8

Kirillov, S., Babb, D. G., Komarov, A. S., Dmitrenko, I., Ehn, J. K., Worden, E., Candlish, L., Rysgaard, S., & Barber, D. G. (2021). On the Physical Settings of Ice Bridge Formation in Nares Strait. *J. Geophys. Res. Ocean.*, *126*(8), 1–19. https://doi.org/10.1029/2021JC017331

Korosov, A., Rampal, P., Toudal Pedersen, L., Saldo, R., Ye, Y., Heygster, G., Lavergne, T., Aaboe, S., & Girard-Ardhuin, F. (2018). A new tracking algorithm for sea ice age distribution estimation. *Cryosphere*, *12*(6), 2073–2085. https://doi.org/10.5194/tc-12-2073-2018

Krishfield, R. A., Proshutinsky, A., Tateyama, K., Williams, W. J., Carmack, E. C., McLaughlin, F. A., & Timmermans, M.-L. (2014). Deterioration of perennial sea ice in the Beaufort Gyre from 2003 to 2012 and its impact on the oceanic freshwater cycle. *J. Geophys. Res. Ocean.*, *119*, 35. https://doi.org/10.1002/2013JC008999

Krumpen, T., Belter, H. J., Boetius, A., Damm, E., Haas, C., Hendricks, S., Nicolaus, M., Nöthig, E., Paul, S., Peeken, I., Ricker, R., & Stein, R. (2019). Arctic warming interrupts the

Transpolar Drift and affects long- range transport of sea ice and ice- rafted matter. *Nat. Sci. Reports*, *9*(March), 1–9. https://doi.org/10.1038/s41598-019-41456-y

Kuang, H., Luo, Y., Ye, Y., Shokr, M., Chen, Z., Wang, S., Hui, F., Bi, H., & Cheng, X. (2022). Arctic Multiyear Ice Areal Flux and Its Connection with Large-Scale Atmospheric Circulations in the Winters of 2002–2021. *Remote Sens.*, *14*(15), 3742. https://doi.org/10.3390/rs14153742

Kwok, R. (2004a). Annual cycles of multiyear sea ice coverage of the Arctic Ocean: 1999-2003. *J. Geophys. Res. Ocean.*, *109*(11), 1999–2003. https://doi.org/10.1029/2003JC002238

Kwok, R. (2004b). Fram Strait sea ice outflow. *J. Geophys. Res.*, *109*(C1), C01009. https://doi.org/10.1029/2003JC001785

Kwok, R. (2005). Variability of Nares Strait ice flux. *Geophys. Res. Lett.*, *32*(24), 1–4. https://doi.org/10.1029/2005GL024768

Kwok, R. (2006). Exchange of sea ice between the Arctic Ocean and the Canadian Arctic Archipelago. *Geophys. Res. Lett.*, *33*(16), 1–5. https://doi.org/10.1029/2006GL027094

Kwok, R. (2007). Near zero replenishment of the Arctic multiyear sea ice cover at the end of 2005 summer. *Geophys. Res. Lett.*, *34*(5), 1–6. https://doi.org/10.1029/2006GL028737

Kwok, R. (2009). Outflow of Arctic Ocean sea ice into the Greenland and Barent Seas: 1979-2007. *J. Clim.*, *22*(9), 2438–2457. https://doi.org/10.1175/2008JCLI2819.1

Kwok, R. (2015). Sea ice convergance along the Arctic coasts of Greenland and the Canadian Arctic Archipelago: Variability and extremes (1992-2014). *Geophys. Res. Lett.*, *42*, 1–8. https://doi.org/10.1002/2015GL065462

Kwok, R. (2018). Arctic sea ice thickness, volume , and multiyear ice coverage: losses and coupled variability (1958 – 2018). *Environ. Res. Lett.*, *13*(10), 105005. https://doi.org/10.1088/1748-9326/aae3ec

Kwok, R., & Cunningham, G. F. (2010). Contribution of melt in the Beaufort Sea to the decline in Arctic multiyear sea ice coverage: 1993-2009. *Geophys. Res. Lett.*, *37*(20), 1–5. https://doi.org/10.1029/2010GL044678

Kwok, R., & Cunningham, G. F. (2015). Variability of arctic sea ice thickness and volume from CryoSat-2. *Philos. Trans. R. Soc. A Math. Phys. Eng. Sci.*, *373*(2045). https://doi.org/10.1098/rsta.2014.0157

Kwok, R., Cunningham, G. F., Wensnahan, M., Rigor, I. G., Zwally, H. J., & Yi, D. (2009). Thinning and volume loss of the Arctic Ocean sea ice cover: 2003-2008. *J. Geophys. Res. Ocean.*, *114*(7), 1–16. https://doi.org/10.1029/2009JC005312

Kwok, R., Maslowski, W., & Laxon, S. W. (2005). On large outflows of Arctic sea ice into the Barents Sea. *Geophys. Res. Lett.*, *32*(22), 1–5. https://doi.org/10.1029/2005GL024485

Kwok, R., Pedersen, L. T., Gudmandsen, P., & Pang, S. S. (2010). Large sea ice outflow into the Nares Strait in 2007. *Geophys. Res. Lett.*, *37*(3). https://doi.org/10.1029/2009GL041872

Kwok, R., & Rothrock, D. A. (2009). Decline in Arctic sea ice thickness from submarine and ICESat records: 1958-2008. *Geophys. Res. Lett.*, *36*(15), 1–5. https://doi.org/10.1029/2009GL039035

Kwok, R., Spreen, G., & Pang, S. (2013). Arctic sea ice circulation and drift speed: Decadal trends and ocean currents. *J. Geophys. Res. Ocean.*, *118*(5), 2408–2425. https://doi.org/10.1002/jgrc.20191

Lindsay, R. W., & Zhang, J. (2005). The thinning of Arctic sea ice, 1988-2003: Have we

passed a tipping point? *J. Clim.*, *18*(22), 4879–4894. https://doi.org/10.1175/JCLI3587.1

Lindsay, R. W., Zhang, J., Schweiger, A., Steele, M., & Stern, H. (2009). Arctic sea ice retreat in 2007 follows thinning trend. *J. Clim.*, *22*(1), 165–176. https://doi.org/10.1175/2008JCLI2521.1

Mahoney, A. R., Hutchings, J. K., Eicken, H., & Haas, C. (2019). Changes in the Thickness and Circulation of Multiyear Ice in the Beaufort Gyre Determined From Pseudo-Lagrangian Methods from 2003–2015. *J. Geophys. Res. Ocean.*, *124*(8), 5618–5633. https://doi.org/10.1029/2018JC014911

Mallett, R. D. C., Stroeve, J. C., Cornish, S. B., Crawford, A. D., Lukovich, J. V., Serreze, M. C., Barrett, A. P., Meier, W. N., Heorton, H. D. B. S., & Tsamados, M. (2021). Record winter winds in 2020/21 drove exceptional Arctic sea ice transport. *Commun. Earth Environ.*, *2*(1), 17–22. https://doi.org/10.1038/s43247-021-00221-8

Maslanik, J. A., Fowler, C., Stroeve, J. C., Drobot, S., Zwally, J., Yi, D., & Emery, W. (2007). A younger, thinner Arctic ice cover: Increased potential for rapid, extensive sea-ice loss. *Geophys. Res. Lett.*, *34*(24), 2004–2008. https://doi.org/10.1029/2007GL032043

Maslanik, J. A., Stroeve, J. C., Fowler, C., & Emery, W. (2011). Distribution and trends in Arctic sea ice age through spring 2011. *Geophys. Res. Lett.*, *38*(13), 2–7. https://doi.org/10.1029/2011GL047735

Meier, W. N., Perovich, D. K., Farrell, S. L., Haas, C., Hendricks, S., Petty, A. A., Webster, M. A., Divine, D. V., Gerland, S., Kaleschke, L., Ricker, R., Steer, A., Tian-Kunze, X., Tschudi, M. A., & Wood, K. R. (2021). *Sea Ice [in 'State of the Climate in 2021"]*. https://doi.org/https://doi. org/10.1175/BAMS-D-22-0082.1.

Meier, W., & Stewart, J. S. (2023). Early EASE-GRID Sea Ice Age, 1978-1983. *Cryosph.*, *14*, 1519–1536. https://doi.org/10.5067/INAWUWO7QH7B

Melling, H. (2002). Sea ice of the northern Canadian Arctic Archipelago. *J. Geophys. Res.*, *107*(C11), 3181. https://doi.org/10.1029/2001JC001102

Meredith, M., Sommerkorn, M., Cassotta, S., Derksen, C., Ekaykin, A., Hollowed, A., Kofinas, G., Mackintosh, A., Melbourne-Thomas, J., Muelbert, M. M. C., Ottersen, G., Pritchard, H., & Schuur, E. A. G. (2019). Polar Regions. In H.-O. P□rtner, D. C. Roberts, V. Masson-Delmotte, P. Zhai, M. Tignor, E. Poloczanska, K. Mintenbeck, A. Alegr□a, M. Nicolai, A. Okem, J. Petzold, B. Rama, & N. M. Weyer (Eds.), *IPCC Special Report on the Ocean and Cryosphere in a Changing Climate* (p. 118).

Moore, G. W. K., Howell, S. E. L., & Brady, M. (2021). First Observations of a Transient Polynya in the Last Ice Area North of Ellesmere Island. *Geophys. Res. Lett.*, *n/a*(n/a), e2021GL095099. https://doi.org/https://doi.org/10.1029/2021GL095099

Moore, G. W. K., Howell, S. E. L., Brady, M., Xu, X., & McNeil, K. (2021). Anomalous collapses of Nares Strait ice arches leads to enhanced export of Arctic sea ice. *Nat. Commun.*, *12*(1), 1–8. https://doi.org/10.1038/s41467-020-20314-w

Moore, G. W. K., Schweiger, A., Zhang, J., & Steele, M. (2019). Spatiotemporal Variability of Sea Ice in the Arctic's Last Ice Area. *Geophys. Res. Lett.*, *46*(20), 11237–11243. https://doi.org/10.1029/2019GL083722

Nghiem, S. V., Chao, Y., Neumann, G., Li, P., Perovich, D. K., Street, T., & Clemente-Colón, P. (2006). Depletion of perennial sea ice in the East Arctic Ocean. *Geophys. Res. Lett.*, *33*(17), 1–6. https://doi.org/10.1029/2006GL027198

Nghiem, S. V., Neumann, G., Rigor, I. G., Clemente-colón, P., & Perovich, D. K. (2011). Arctic

Perennial Sea Ice Crash of the 2000s and its Impacts. *BIONATURE 2011 Second. Int. Conf. Bioenvironment, Biodivers. Renew. Energies*, *March 2007*, 38–42.

Nghiem, S. V., Rigor, I. G., Perovich, D. K., Clemente-Colón, P., Weatherly, J. W., & Neumann, G. (2007). Rapid reduction of Arctic perennial sea ice. *Geophys. Res. Lett.*, *34*(19), 1–6. https://doi.org/10.1029/2007GL031138

Notz, D. (2009). The future of ice sheets and sea ice: Between reversible retreat and unstoppable loss. *Proc. Natl. Acad. Sci. U. S. A.*, *106*(49), 20590–20595. https://doi.org/10.1073/pnas.0902356106

Perovich, D. K., & Polashenski, C. (2012). Albedo evolution of seasonal Arctic sea ice. *Geophys. Res. Lett.*, *39*(8), 1–6. https://doi.org/10.1029/2012GL051432

Perovich, D. K., Richeter-Menge, J. A., Jones, K. F., & Light, B. (2008). Sunlight, water, and ice: Extreme Arctic sea ice melt during the summer of 2007. *Geophys. Res. Lett.*, *35*(11), 2–5. https://doi.org/10.1029/2008GL034007

Petty, A. A., Holland, M. M., Bailey, D. A., & Kurtz, N. T. (2018). Warm Arctic, Increased Winter Sea Ice Growth? *Geophys. Res. Lett.*, *45*(23), 12,922-12,930. https://doi.org/10.1029/2018GL079223

Petty, A. A., Keeney, N., Cabaj, A., Kushner, P., & Bagnardi, M. (2023). Winter Arctic sea ice thickness from ICESat-2: upgrades to freeboard and snow loading estimates and an assessment of the first three winters of data collection. *Cryosphere*, *17*(1), 127–156. https://doi.org/10.5194/tc-17-127-2023

Pfirman, S., Haxby, W. F., Colony, R., & Rigor, I. G. (2004). Variability in Arctic sea ice drift. *Geophys. Res. Lett.*, *31*(16), 1–4. https://doi.org/10.1029/2004GL020063

Pizzolato, L., Howell, S. E. L., Derksen, C., Dawson, J., & Copland, L. (2014). Changing sea ice conditions and marine transportation activity in Canadian Arctic waters between 1990 and 2012. *Clim. Change*, *123*(2), 161–173. https://doi.org/10.1007/s10584-013-1038-3

Rampal, P., Weiss, J., & Marsan, D. (2009). Positive trend in the mean speed and deformation rate of Arctic sea ice, 1979-2007. *J. Geophys. Res. Ocean.*, *114*(5), 1–14. https://doi.org/10.1029/2008JC005066

Regan, H. C., Rampal, P., Ólason, E., Boutin, G., & Korosov, A. (2023). Modelling the evolution of Arctic multiyear sea ice over 2000-2018. *Cryosph. Discuss.*, *November*, 1–28. https://doi.org/https://doi.org/10.5194/tc-17-1873-2023

Ricker, R., Girard-Ardhuin, F., Krumpen, T., & Lique, C. (2018). Satellite-derived sea ice export and its impact on Arctic ice mass balance. *Cryosph.*, *12*(9), 3017–3032. https://doi.org/10.5194/tc-12-3017-2018

Ricker, R., Hendricks, S., Girard-Ardhuin, F., Kaleschke, L., Lique, C., Tian-Kunze, X., Nicolaus, M., & Krumpen, T. (2017). Satellite-observed drop of Arctic sea ice growth in winter 2015–2016. *Geophys. Res. Lett.*, *44*(7), 3236–3245. https://doi.org/10.1002/2016GL072244

Ricker, R., Kauker, F., Schweiger, A., Hendricks, S., Zhang, J., & Paul, S. (2021). Evidence for an increasing role of ocean heat in arctic winter sea ice growth. *J. Clim.*, *34*(13), 5215–5227. https://doi.org/10.1175/JCLI-D-20-0848.1

Rigor, I. G., & Wallace, J. M. (2004). Variations in the age of Arctic sea-ice and summer sea-ice extent. *Geophys. Res. Lett.*, *31*(9), 2–5. https://doi.org/10.1029/2004GL019492

Rigor, I. G., Wallace, J. M., & Colony, R. L. (2002). Response of sea ice to the Arctic Oscillation. *J. Clim.*, *15*, 2648–2663. https://doi.org/10.1175/1520-

0442(2002)015<2648:ROSITT>2.0.CO;2
Rothrock, D. A., Yu, Y., & Maykut, G. A. (1999). Thinning of the Arctic Sea-Ice cover. *Geophys. Res. Lett.*, *26*(23), 3469–3472. https://doi.org/10.1029/1999GL010863
Schweiger, A. J., Steele, M., Zhang, J., Moore, G. W. K., & Laidre, K. L. (2021). Accelerated sea ice loss in the Wandel Sea points to a change in the Arctic's Last Ice Area. *Commun. Earth Environ.*, *2*(1), 122. https://doi.org/10.1038/s43247-021-00197-5
Shokr, M., Lambe, A., & Agnew, T. (2008). A New Algorithm (ECICE) to Estimate Ice Concentration From Remote Sensing Observations: An Application to 85-GHz Passive Microwave Data. *IEEE Trans. Geosci. Remote Sens.*, *46*(12), 4104–4121. https://doi.org/10.1109/TGRS.2008.2000624
SIMIP Community. (2020). Arctic Sea Ice in CMIP6. *Geophys. Res. Lett.*, *47*(10). https://doi.org/10.1029/2019gl086749
Smedsrud, L. H., Halvorsen, M. H., Stroeve, J. C., Zhang, R., & Kloster, K. (2017). Fram Strait sea ice export variability and September Arctic sea ice extent over the last 80 years. *Cryosphere*, *11*(1), 65–79. https://doi.org/10.5194/tc-11-65-2017
Stroeve, J. C., Schroder, D., Tsamados, M., & Feltham, D. (2018). Warm winter, thin ice? *Cryosphere*, *12*(5), 1791–1809. https://doi.org/10.5194/tc-12-1791-2018
Stroeve, J., & Notz, D. (2018). Changing state of Arctic sea ice across all seasons. *Environ. Res. Lett.*, *13*(10). https://doi.org/10.1088/1748-9326/aade56
Sumata, H., de Steur, L., Divine, D. V., Granskog, M. A., & Gerland, S. (2023). Regime shift in Arctic Ocean sea ice thickness. *Nature*, *615*(7952), 443–449. https://doi.org/10.1038/s41586-022-05686-x
Sumata, H., de Steur, L., Gerland, S., Divine, D. V., & Pavlova, O. (2022). Unprecedented decline of Arctic sea ice outflow in 2018. *Nat. Commun.*, *13*(1). https://doi.org/10.1038/s41467-022-29470-7
Thomas, D. R., & Rothrock, D. A. (1993). The Arctic Ocean ice balance: A Kalman smoother estimate. *J. Geophys. Res.*, *98*(C6), 10053. https://doi.org/10.1029/93JC00139
Tilling, R. L., Ridout, A., Shepherd, A., & Wingham, D. J. (2015). Increased Arctic sea ice volume after anomalously low melting in 2013. *Nat. Geosci.*, *8*(August), 643–646. https://doi.org/10.1038/NGEO2489
Tschudi, M. A., Meier, W. N., Stewart, J. S., Fowler, C., & Maslanik, J. A. (2019a). *EASE-Grid Sea Ice Age, Version 4*. https://doi.org/https://doi.org/10.5067/UTAV7490FEPB
Tschudi, M. A., Meier, W. N., Stewart, J. S., Fowler, C., & Maslanik, J. A. (2019b). *Polar Pathfinder Daily 25 km EASE-Grid Sea Ice Motion Vectors, Version 4*. https://doi.org/https://doi.org/10.5067/INAWUWO7QH7B
Tschudi, M. A., Stroeve, J. C., & Stewart, J. S. (2016). Relating the age of Arctic sea ice to its thickness, as measured during nasa's ICESat and IceBridge campaigns. *Remote Sens.*, *8*(6). https://doi.org/10.3390/rs8060457
Vincent, R. F. (2019). A Study of the North Water Polynya Ice Arch using Four Decades of Satellite Data. *Sci. Rep.*, *9*(1), 1–12. https://doi.org/10.1038/s41598-019-56780-6
Wang, Y., Bi, H., & Liang, Y. (2022). A Satellite-Observed Substantial Decrease in Multiyear Ice Area Export through the Fram Strait over the Last Decade. *Remote Sens.*, *14*(11), 2562. https://doi.org/10.3390/rs14112562
Ye, Y., Luo, Y., Sun, Y., Shokr, M., Aaboe, S., Girard-Ardhuin, F., Hui, F., Cheng, X., & Chen, Z. (2023). Inter-comparison and evaluation of Arctic sea ice type products. *Cryosphere*, *17*(1), 279–308. https://doi.org/10.5194/tc-17-279-2023

Supplementary Figures

Figure S1: Plots of the annual MYI Budget for the Arctic Ocean from 1985 - 2021. The terms of Export, Melt and Replenishment, along with the error that accumulates during freeze up are given in each panel. The error is given as both a magnitude of area and percentage of the true maximum area.

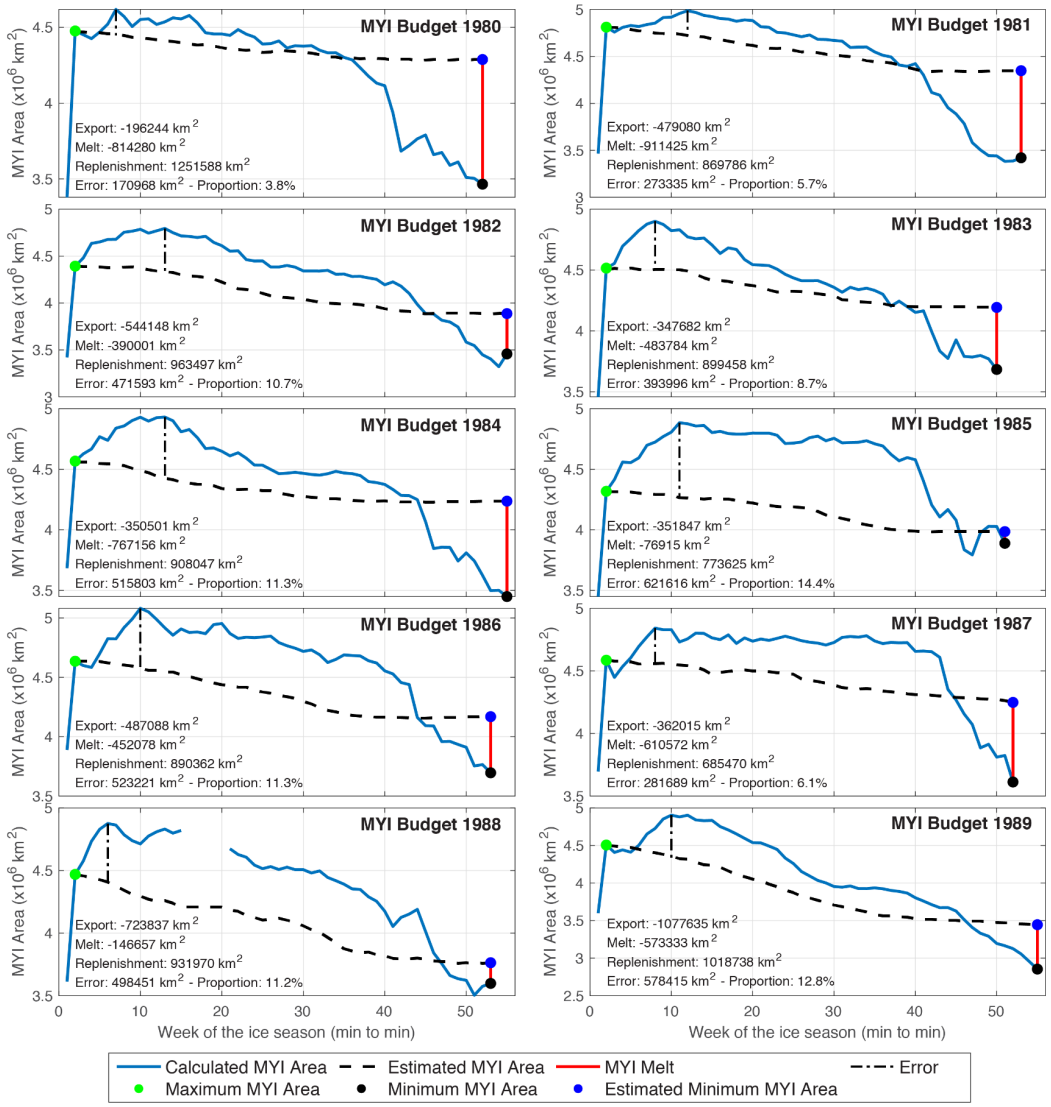

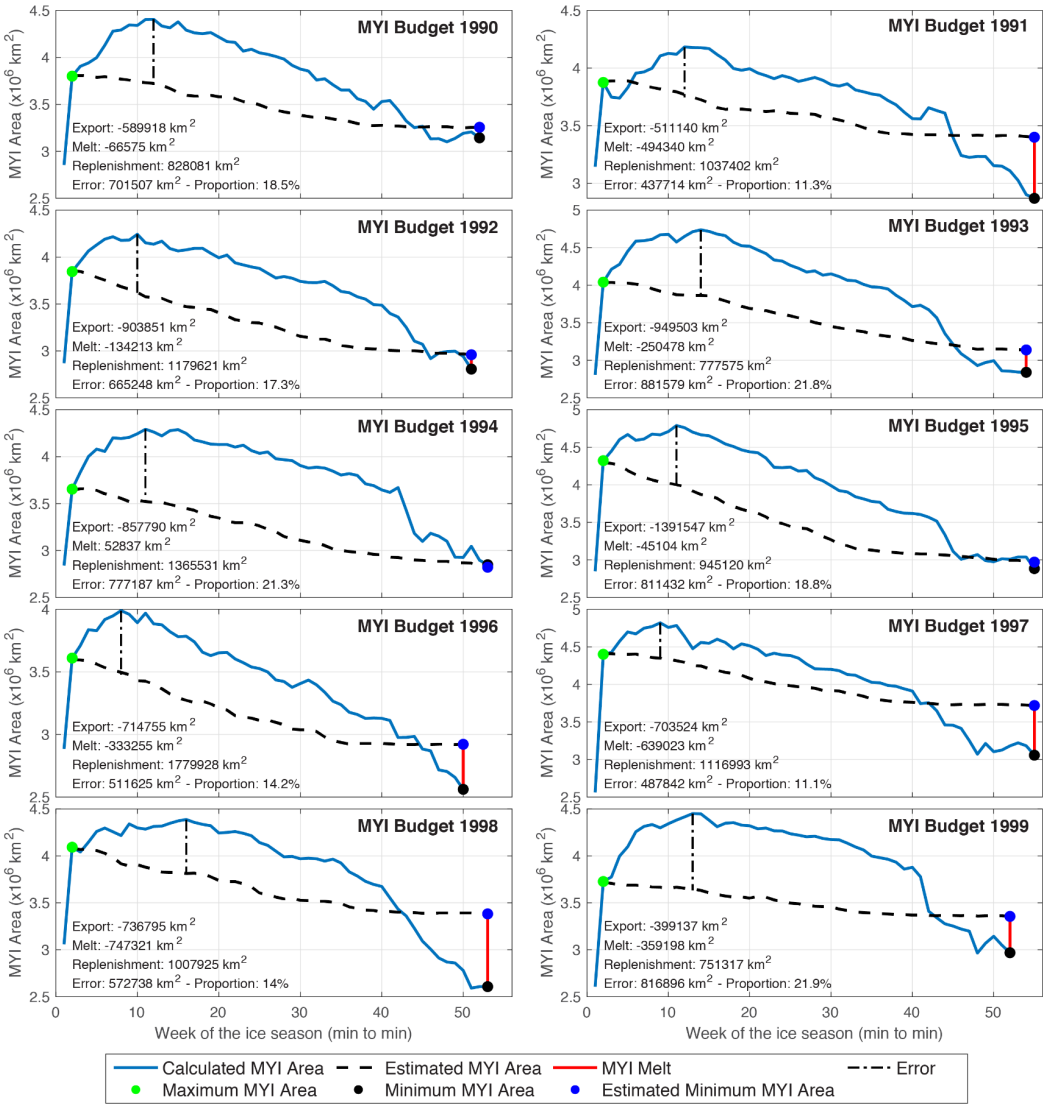
MYI Budget 1990
Export: -589918 km 2
Melt: -66575 km 2
Replenishment: 828081 km2
Error: 701507 km2 - Proportion: 18.5%
MYI Budget 1991
Export: -511140 km 2
Melt: -494340 km 2
Replenishment: 1037402 km2
Error: 437714 km2 - Proportion: 11.3%
MYI Budget 1992
Export: -903851 km 2
Melt: -134213 km 2
Replenishment: 1179621 km2
Error: 665248 km2 - Proportion: 17.3%
MYI Budget 1993
Export: -949503 km 2
Melt: -250478 km 2
Replenishment: 777575 km2
Error: 881579 km2 - Proportion: 21.8%
MYI Budget 1994
Export: -857790 km 2
Melt: 52837 km 2
Replenishment: 1365531 km2
Error: 777187 km2 - Proportion: 21.3%
MYI Budget 1995
Export: -1391547 km 2
Melt: -45104 km 2
Replenishment: 945120 km2
Error: 811432 km2 - Proportion: 18.8%
MYI Budget 1996
Export: -714755 km 2
Melt: -333255 km 2
Replenishment: 1779928 km2
Error: 511625 km2 - Proportion: 14.2%
MYI Budget 1997
Export: -703524 km 2
Melt: -639023 km 2
Replenishment: 1116993 km2
Error: 487842 km2 - Proportion: 11.1%
MYI Budget 1998
Export: -736795 km 2
Melt: -747321 km 2
Replenishment: 1007925 km2
Error: 572738 km2 - Proportion: 14%
MYI Budget 1999
Export: -399137 km 2
Melt: -359198 km 2
Replenishment: 751317 km2
Error: 816896 km2 - Proportion: 21.9%
MYI Area (x10^6 km^2)
Week of the ice season (min to min)
Calculated MYI Area
Estimated MYI Area
MYI Melt
Error
Maximum MYI Area
Minimum MYI Area
Estimated Minimum MYI Area

1117

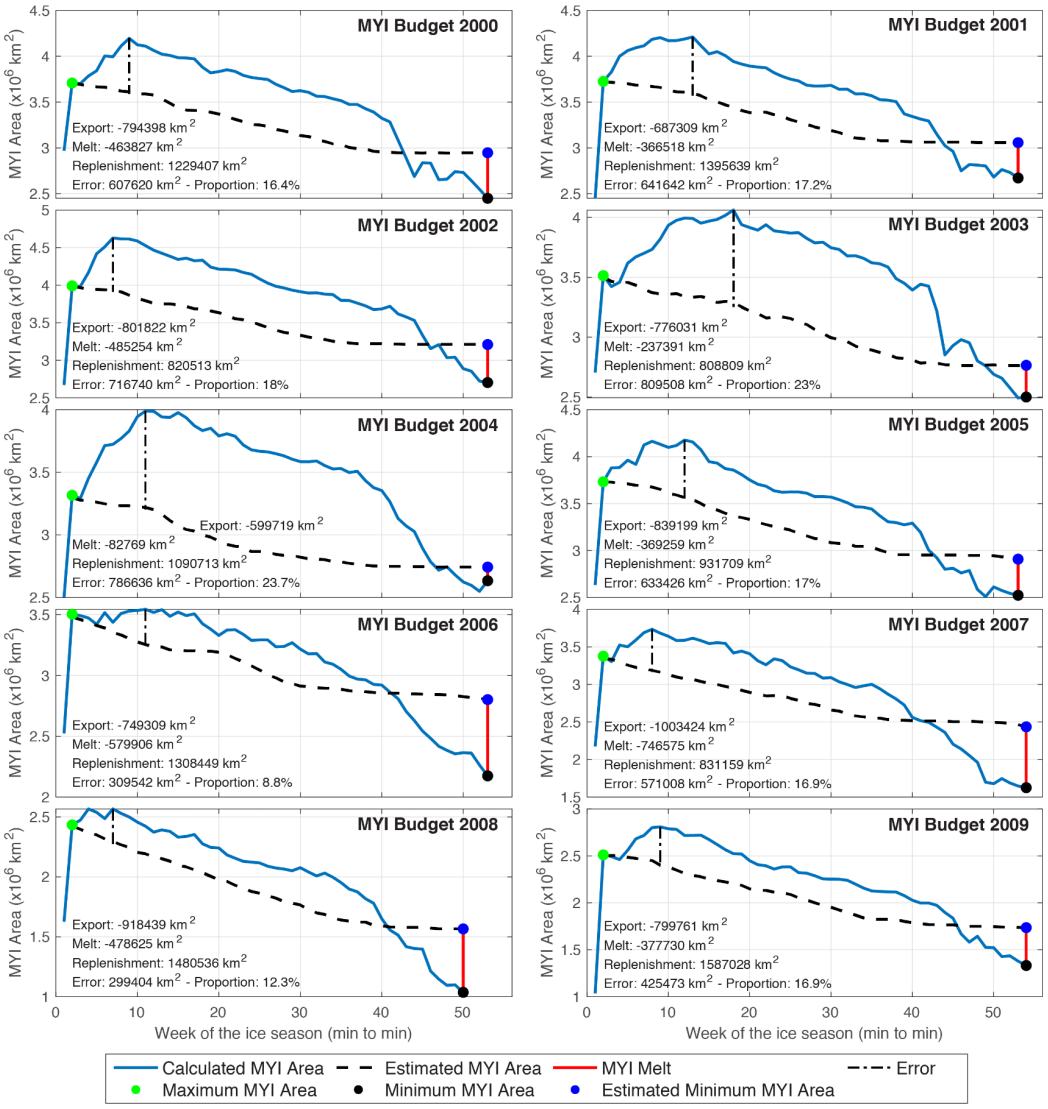
MYI Budget 2000
Export: -794398 km 2
Melt: -463827 km 2
Replenishment: 1229407 km 2
Error: 607620 km 2 - Proportion: 16.4%
MYI Budget 2001
Export: -687309 km 2
Melt: -366518 km 2
Replenishment: 1395639 km 2
Error: 641642 km 2 - Proportion: 17.2%
MYI Budget 2002
Export: -801822 km 2
Melt: -485254 km 2
Replenishment: 820513 km 2
Error: 716740 km 2 - Proportion: 18%
MYI Budget 2003
Export: -776031 km 2
Melt: -237391 km 2
Replenishment: 808809 km 2
Error: 809508 km 2 - Proportion: 23%
MYI Budget 2004
Export: -599719 km 2
Melt: -82769 km 2
Replenishment: 1090713 km 2
Error: 786636 km 2 - Proportion: 23.7%
MYI Budget 2005
Export: -839199 km 2
Melt: -369259 km 2
Replenishment: 931709 km 2
Error: 633426 km 2 - Proportion: 17%
MYI Budget 2006
Export: -749309 km 2
Melt: -579906 km 2
Replenishment: 1308449 km 2
Error: 309542 km 2 - Proportion: 8.8%
MYI Budget 2007
Export: -1003424 km 2
Melt: -746575 km 2
Replenishment: 831159 km 2
Error: 571008 km 2 - Proportion: 16.9%
MYI Budget 2008
Export: -918439 km 2
Melt: -478625 km 2
Replenishment: 1480536 km 2
Error: 299404 km 2 - Proportion: 12.3%
MYI Budget 2009
Export: -799761 km 2
Melt: -377730 km 2
Replenishment: 1587028 km 2
Error: 425473 km 2 - Proportion: 16.9%
MYI Area (x10 6 km 2)
Week of the ice season (min to min)
Calculated MYI Area
Estimated MYI Area
MYI Melt
Error
Maximum MYI Area
Minimum MYI Area
Estimated Minimum MYI Area

1118

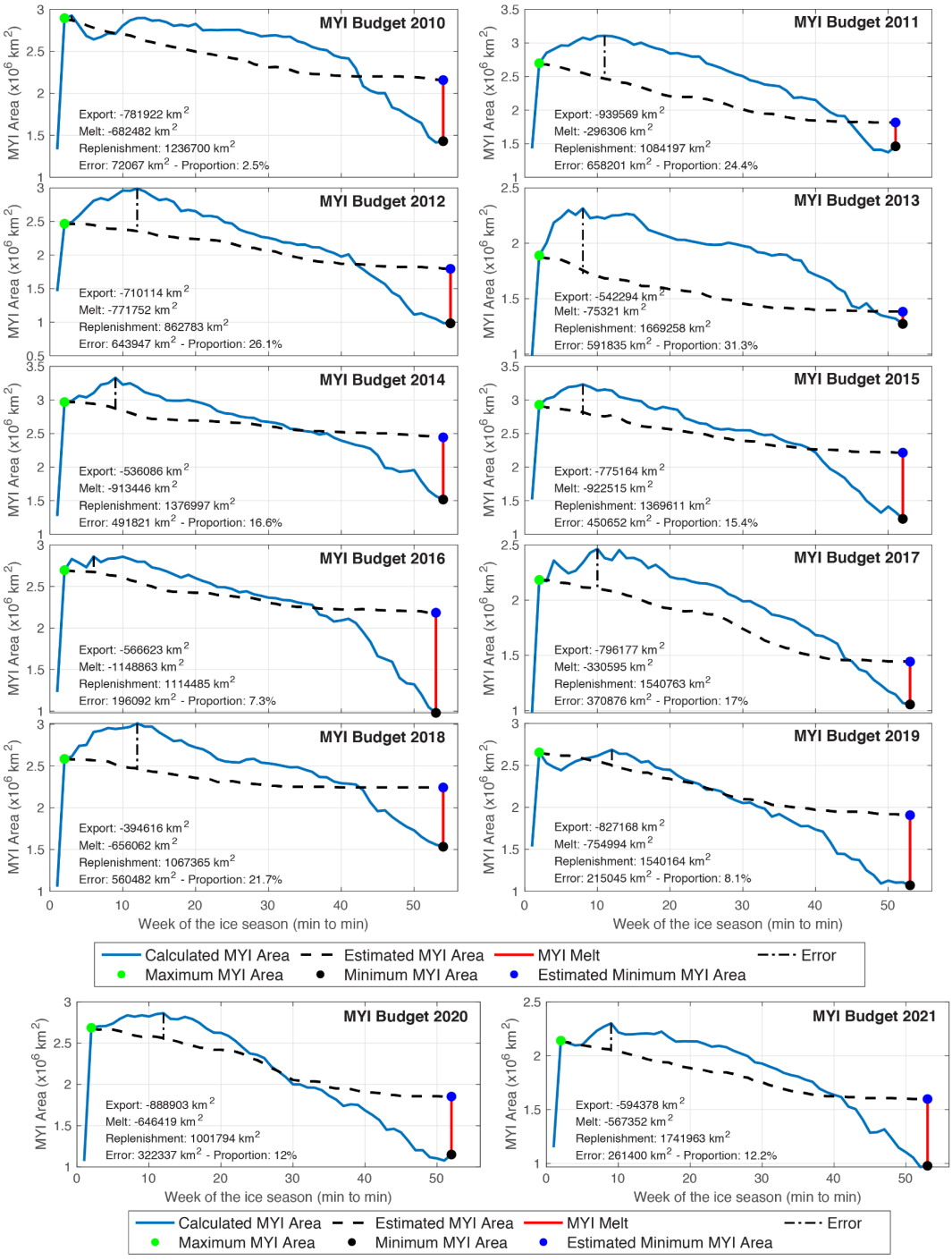
MYI Budget 2010
Export: -781922 km²
Melt: -682482 km²
Replenishment: 1236700 km²
Error: 72067 km² - Proportion: 2.5%
MYI Budget 2011
Export: -939569 km²
Melt: -296306 km²
Replenishment: 1084197 km²
Error: 658201 km² - Proportion: 24.4%
MYI Budget 2012
Export: -710114 km²
Melt: -771752 km²
Replenishment: 862783 km²
Error: 643947 km² - Proportion: 26.1%
MYI Budget 2013
Export: -542294 km²
Melt: -75321 km²
Replenishment: 1669258 km²
Error: 591835 km² - Proportion: 31.3%
MYI Budget 2014
Export: -536086 km²
Melt: -913446 km²
Replenishment: 1376997 km²
Error: 491821 km² - Proportion: 16.6%
MYI Budget 2015
Export: -775164 km²
Melt: -922515 km²
Replenishment: 1369611 km²
Error: 450652 km² - Proportion: 15.4%
MYI Budget 2016
Export: -566623 km²
Melt: -1148863 km²
Replenishment: 1114485 km²
Error: 196092 km² - Proportion: 7.3%
MYI Budget 2017
Export: -796177 km²
Melt: -330595 km²
Replenishment: 1540763 km²
Error: 370876 km² - Proportion: 17%
MYI Budget 2018
Export: -394616 km²
Melt: -656062 km²
Replenishment: 1067365 km²
Error: 560482 km² - Proportion: 21.7%
MYI Budget 2019
Export: -827168 km²
Melt: -754994 km²
Replenishment: 1540164 km²
Error: 215045 km² - Proportion: 8.1%
MYI Area (x10⁶ km²)
Week of the ice season (min to min)
Calculated MYI Area
Estimated MYI Area
MYI Melt
Error
Maximum MYI Area
Minimum MYI Area
Estimated Minimum MYI Area
MYI Budget 2020
Export: -888903 km²
Melt: -646419 km²
Replenishment: 1001794 km²
Error: 322337 km² - Proportion: 12%
MYI Budget 2021
Export: -594378 km²
Melt: -567352 km²
Replenishment: 1741963 km²
Error: 261400 km² - Proportion: 12.2%

Figure S2. Time series of observed and estimated total ice export into Nares Strait from 1979 to 2021. Observed fluxes from Kwok (2005) and Kwok et al. (2010) are in blue, and Moore et al. (2021) are in red. Estimates based on the relationship between open water duration and total ice flux (F = 285.74 * *duration* – 19577) are presented in yellow.